2nd Department of Medicine and Cardiology Center, Medical Faculty,
Albert Szent-Györgyi Clinical Center,
University of Szeged

Left ventricular rotational abnormalities in different disorders

Árpád Kormányos MD

PhD thesis

Tutor:

Prof. Attila Nemes MD, PhD, DSc

2019

Relevant publications

Full papers

I. **Kormányos Á**, Kalapos A, Domsik P, Lengyel C, Forster T, Nemes A. Normal values of left ventricular rotational parameters in healthy adults-Insights from the three-dimensional speckle tracking echocardiographic MAGYAR-Healthy Study. Echocardiography. 2019 Apr;36(4):714-21. **(impact factor: 1.287)**

II. **Kormányos Á**, Domsik P, Kalapos A, Orosz A, Lengyel C, Valkusz Z, Trencsányi A, Forster T, Nemes A. Left ventricular twist is impaired in acromegaly: Insights from the three-dimensional speckle tracking echocardiographic MAGYAR-Path Study. J Clin Ultrasound. 2018 Feb;46(2):122-8. **(impact factor: 0.820)**

III. Borda B, **Kormányos Á**, Domsik P, Kalapos A, Lengyel C, Ambrus N, Lázár G, Forster T, Nemes A. Left ventricular rotational abnormalities following successful kidney transplantation-insights from the three-dimensional speckle-tracking echocardiographic MAGYAR-Path Study. Quant Imaging Med Surg. 2018 Dec;8(11):1095-101. **(impact factor: 3.074)**

IV. Nemes A, **Kormányos Á**, Domsik P, Kalapos A, Kemény L, Forster T, Szolnoky G. Left ventricular rotational mechanics differ between lipedema and lymphedema: Insights from the three-dimensional speckle tracking echocardiographic MAGYAR-Path Study. Lymphology. 2018;51(3):102-8. **(impact factor: 0. 674)**

V. **Kormányos Á**, Domsik P, Kalapos A, Marton I, Földeák D, Modok S, Gyenes N, Borbényi Z, Nemes A. Left ventricular deformation in cardiac AL amyloidosis and hypereosinophilic syndrome (Results from the MAGYAR-Path Study) Orv Hetil. *in press*. **(impact factor: 0.564)**

Table of contents

Abbreviations

2DE = two-dimensional echocardiogrpahy

2DSTE = two-dimensional speckle tracking echocardiography

3DEDV = three-dimensional end-diastolic volume

3DEF = three-dimensional ejection fracture

3DESV = three-dimensional end-systolic volume

3DLVM= three-dimensional left ventricular mass

3DS = three-dimensional strain

3DSTE = three-dimensional speckle tracking echocardiography

A = late-filling transmitral flow velocity

ALA = immunglobulin light chain amyloidosis

AP2CH = apical two chamber view

AP4CH = apical four chamber view

AS = area strain

BMI = body mass index

cMRI = cardiac magnetic resonance imaging

CKD = chronic kidney disease

CVD = cardiovascular disease

CS = circumferential strain

E = early-filling transmitral flow velocity

ECG = electrocardiography

EDD = end-diastolic diameter

EDV = end-diastolic volume

EF = ejection fraction

ESRD = end-stage renal disease

GH = growth hormone

HES = hypereosinophilic syndrome

IGF-1 = insulin like growth factor-1

KTx = kidney transplant

LA = left atrium

LS = longitudinal strain

LV = left ventricle

NCCMP = non-compaction cardiomyopathy

RBR = rigid body rotation

RS = radial strain

TDI = tissue Doppler imaging

1. Introduction

Echocardiography is a widely used method of choice in assessing different cardiac functions (1). *Three-dimensional speckle tracking echocardiography (3DSTE)* is a new non-invasive tool, which provides a new method to simultaneously assess the heart as a whole coordinated unit, and to quantify the complex motions of different heart chambers. Using 3DSTE, it is possible to reliably assess cardiac mechanics including LV volumetric, strain and rotational analysis at the same time from the same digitally stored dataset (2) as validated against both sonomicrometry and two-dimensional speckle tracking echocardiography (2DSTE) (3, 4).

The complex myocardial mechanics that is called *left ventricular (LV) twist* has been known since Leonardo Da Vinci (5). This "towel wringing" motion of the LV is due to a very special myocardial anatomy. The LV is comprised of a subendocardial oblique layer with right-handed helix having a smaller radius and a subepicardial oblique left-handed helix layer with a larger radius. This architecture results in the clockwise rotation of the LV base and the counter-clockwise rotation of the LV apex, and their net difference is the so-called LV twist (6-11). The physiological importance of this phenomenon is well understood, however its clinical implication is still not well documented (10). In some special circumstances the near absence of LV twist could be demonstrated when apical and basal rotations move in the same direction. This sort of movement is called LV 'rigid body rotation' (RBR) (12, 13). To the best of the authors knowledge, there are a limited number of studies using 3DSTE to quantify LV rotational mechanics in *healthy adults* (14), also there are no studies examining gender-dependency of LV rotational mechanics and twist using 3DSTE.

Acromegaly is a rare, chronic, disfiguring and debilitating disease caused by a benign monoclonal growth hormone (GH) secreting pituitary adenoma in 90% of the cases (15). The excessive amount of GH and consequently elevated levels of insulin like growth factor–1 (IGF-1) entail a wide range of clinical symptoms and co-existing illnesses including cardiovascular, endocrine, respiratory and metabolic morbidities(16). Cardiovascular involvement can be seen in 60% of acromegalics and it entails hypertension, concentric left ventricular hypertrophy, heart failure, aortic and mitral valve regurgitation. In rare cases arrhythmias and sudden death may develop (17). The severity of these cardiac complications is directly related to the overall duration of elevated GH secretion, rather than GH or IGF-1 levels themselves (18, 19). LV rotational mechanics in acromegaly has not been previously assessed using 3DSTE.

Kidney transplantation (KTx) is the preferred treatment for virtually all suitable candidates with *end-stage renal disease (ESRD)* (20). Compared to dialysis, KTx improves both survival and quality of the life of the patients. In patients following successful KTx, leading causes of death are cardiovascular diseases (CVDs) (20). Theoretically, early detection of CVD-related alterations in myocardial mechanics could help in the selection of high-risk patients.

Lymphedema is the tissue swelling resulting from excessive accumulation of lymphatic fluid in the interstitial compartment pathophysiologically based on impaired lymphatic conductancy due to mechanical or dynamical causes. Lymphedema is a chronic progressive disease with serious physical and psychosocial implications. If remains untreated connective tissue proliferation and enlargement could be observed and the characteristic pitting edema is converted into non-pitting swelling (21). *Lipedema* is an often underdiagnosed masquerading disease of obesity or primary lymphedema where the underlying causes are barely understood. Clinically, it is a disproportional, bilateral and symmetrical fat deposition developing downward from the hips with disease-free feet and occasional arm affection. It predominantly affects women with a high incidence of familial accumulation and usually appears by the third decade of life. Non-pitting oedema is a striking halmark as well as tenderness, spontaneous or minor trauma induced pain and bruising. Various dietary approaches usually result in poor success rate however lipedema is frequently combined with obesity. The most effective treatment is liposuction although represents a pivotal differential diagnostic point with primary lymphedema, the genetically determined malformation of lymphatic vasculature and/or lymph nodes (22). Theoretically, there could be a cardiovascular adaptation to lipedema/lymphedema-related haemodynamic consequences. However, limited informations are available regarding to these alterations.

Hypereosinophilic syndrome (HES) and acquired systemic *immunglobulin light-chain amyloidosis (ALA)* are two rare, hematologic diseases, which involve the cardiovascular system. HES is a very heterogenous disease group and its exact definition has been debated for decades (23, 24). HES is characterized by persistent, elevated levels of- more than $1{,}5x10^9$/L- absolute eosinophil granulocytes, which results in organ damage (24). Aetiology based classification of HES is possible nowadays thanks to the modern molecular and immunologic diagnostic methods. Idiopathic HES is diagnosed by eliminating primer clonal and secondary reactive diseases that cause hypereosinophilia. Clinically, HES can appear in numerous forms from asymptomatic disease to severe tissue damage and end stage organ failure. The most prominent cause for morbidity and mortality in HES is linked to cardiovascular involvement.

The early necrotic phase begins with eosinophil infiltration and it is followed by an intermedier thrombotic phase and in late stages the cardiovascular involvement is characterized by fibrosis (Löeffler endocarditis) (25-29). Systemic amyloidosis is a rare disease group characterized by extracellular deposition of insoluble protein fibrils. The most common type is ALA, which is the result of clonal plasma proliferation or other B-cell dyscrasia with immunoglobulin secretion. Deposition of amyloid fibrils can affect any organ, and among others, the heart is considered to be the most affected (approximately 50%) (30-33). Clinical manifestations are pronounced in ALA, which may be due to the toxic effect of light chain deposition on myocardial cells. Based on current guidelines, biomarker-, histology-, electrocardiography (ECG), and imaging tests may help in diagnosis (32-36). Myocardial rotational abnormalities are not well established in both HES and ALA.

2. Aims

To detect LV rotational and twist differences across different age groups and genders in a healthy population using 3DSTE.

To assess LV rotational and twist mechanics in acromegaly patients and to compare their results to age- and gender-matched healthy controls.

To examine LV rotational mechanics post-KTx and to compare it to age- and gender-matched healthy controls.

To assess 3DSTE-derived LV rotational mechanics both in lipedema and lymphedema patients and to compare their results to age- and gender-matched healthy controls.

To compare the LV strain parameters and LV rotational mechanics of HES and ALA patients using 3DSTE and to compare their results with age- and gender-matched healthy controls.

3. Methods

Patient population (general considerations). Healthy volunteers assessed to determine normal reference values came from the **MAGYAR-Healthy Study** (**M**otion **A**nalysis of the heart and **G**reat vessels b**Y** three-dimension**A**l speckle-t**R**acking echocardiography in **Healthy subjects**), where 'magyar' means 'Hungarian' in the Hungarian language. This study has been organized to determine normal values of 3DSTE parameters in healthy adults. For pathological states we used data from patients enrolled in the **MAGYAR-Path Study** (Similar to the Healthy substudy but in Pathological cases) which aimed to examine pathophysiological consequences of different pathological states on myocardial mechanics among others. The present study was approved by the institution's human research committee and also complied with the ethical guidelines set by the 1975 Declaration of Helsinki. All patients gave informed consent.

Two-dimensional Doppler and tissue Doppler echocardiography. Two-dimensional echocardiographic (2DE) assessment and measurements were carried out using a Toshiba Artida^{TM} imaging system (Toshiba Medical Systems, Tokyo, Japan) and a PST-30SBP (1-5 MHz) phased- array transducer by experienced operators. Complete 2D Doppler study was performed in all cases followed by the quantification of LV dimensions, volumes and function and left atrial (LA) dimensions according to current clinical standards (37). For valvular regurgitations, visual assessment was used, and to exclude valvular stenosis, Doppler measurements were performed according to guidelines.

Three-dimensional speckle tracking echocardiography-derived left ventricular volumetric and rotational measurements. 3DSTE measurements were carried out using the same Toshiba Artida^{TM} echocardiography equipment (Toshiba Medical Systems, Tokyo, Japan) with PST-25SX matrix-array transducer (Toshiba Medical Systems, Tokyo, Japan) with 3DSTE capability. Full volume 3D datasets were obtained from apical four chamber view (AP4CH) during a single breath hold. The Toshiba software compiles the full volume dataset from 6, smaller, wedge-shaped subvolumes, therefore the measurements require constant RR intervals. Offline image analysis was performed using 3D Wall Motion Tracking software version 2.7 (Toshiba Medical Systems, Tokyo, Japan). The software automatically selects the apical four- and two-chamber (AP2CH) views and also 3 cross sectional views from the pyramidal 3D datasets. To standardize the measurements, the software provides 2 guide planes, one for the LV base and one for LV apex. Measurements were made during a complete heart

cycle. All datasets underwent a thorough quality control, where any datasets were excluded where not all LV segments were correctly visualized during a heart cycle thus significantly reducing reliability of the offline measurement. The following 3DSTE-derived parameters were assessed:

LV volumetric parameters:

- LV end-diastolic and end-systolic volume (3DEDV, 3DESV)
- LV ejection fraction (3DEF)
- LV mass (3DLVM)

LV rotational and twist parameters:

- LV basal rotation (defined as the degree of clockwise rotation of LV basal myocardial segments)
- LV apical rotation (defined as the degree of counter-clockwise rotation of LV apical myocardial segments).
- LV twist (defined as the difference between LV basal and apical rotation)

LV time-to-peak rotational parameters:

- Time to peak degree of LV basal and apical rotation from the start of the heart cycle.
- Time to peak degree of LV twist from the start of the heart cycle.

LV strain parameters:

- Radial strain (thickening-thinning of segment wall, RS)
- Longitudinal strain (segment elongation-shortening in LV longitudinal axis, LS)
- Circumferential strain (segment widening-narrowing along LV wall, CS)
- Area strain (combination of LS and CS, AS)
- Three- dimensional strain (combination of RS, LS and CS, 3DS)

Example measurements are shown on Figure 1, 2 and 3.

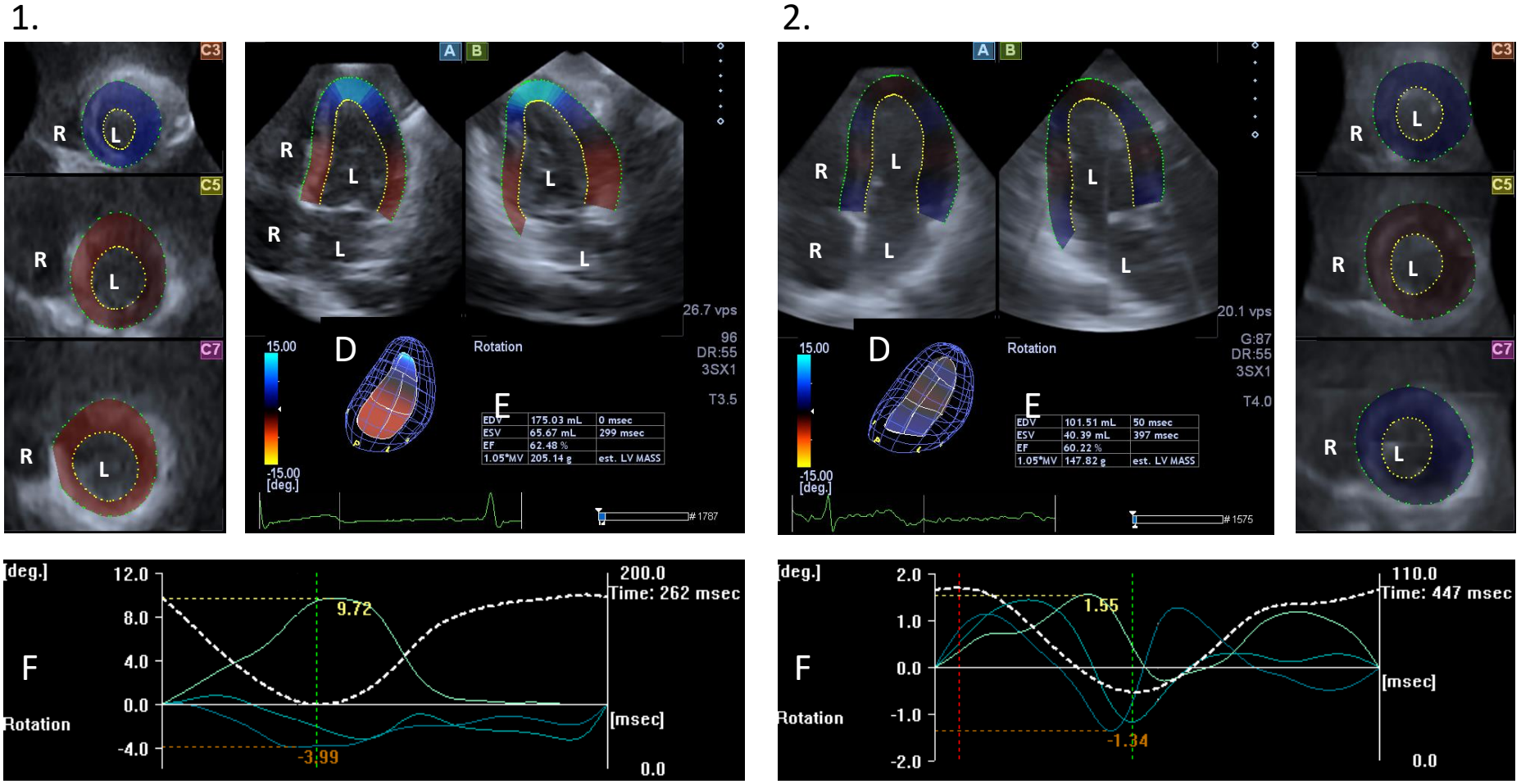

Figure 1. Three-dimensional (3D) speckle-tracking assessment of left ventricular (LV) rotational mechanics is presented in a healthy subject. Panel 1 shows a normal LV rotational pattern, whereas Panel 2 shows the so-called "LV rigid body" rotational pattern. 'A' shows the apical four-chamber view, 'B' demonstrates the apical two-chamber view of the LV, while 'C3-5' are cross sections of the LV. 'D' is the 3D cast of the LV and 'E' shows LV volumetric data corresponding to the measurement. 'F' shows the actual LV apical (white line), midventricular (light blue line) and basal (dark blue line) rotation curves and the volume change of the LV during a heart cycle (dashed line). Abbreviations: LV = left ventricle, RV = right ventricle, LA = left atrium, RA = right atrium.

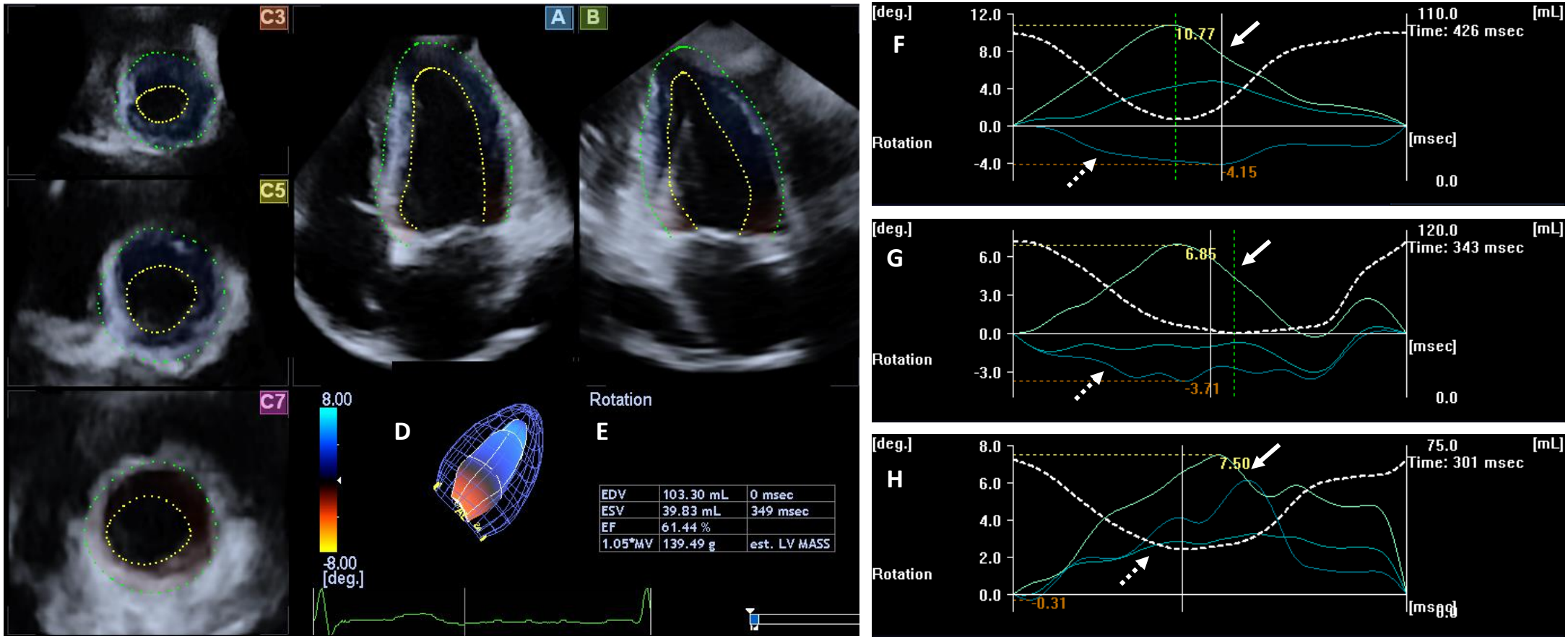

Figure 2. (left:) Apical 4-chamber (A) and 2-chamber (B) views and short-axis views (C3, C5, C7) at different levels of the left ventricle (LV) extracted from the three-dimensional (3D) echocardiographic dataset are presented. The 3D mesh model of the LV (D) and calculated LV volumetric data (E) are also shown. (right:) Images with normal LV rotational pattern with counterclockwise apical (white arrow) and clockwise basal rotations (dashed arrows)(F), apical LV hyporotation (G) and the near absence of LV twist called as LV rigid body rotation with LV apical and basal rotations in the same direction (H) are presented

1.

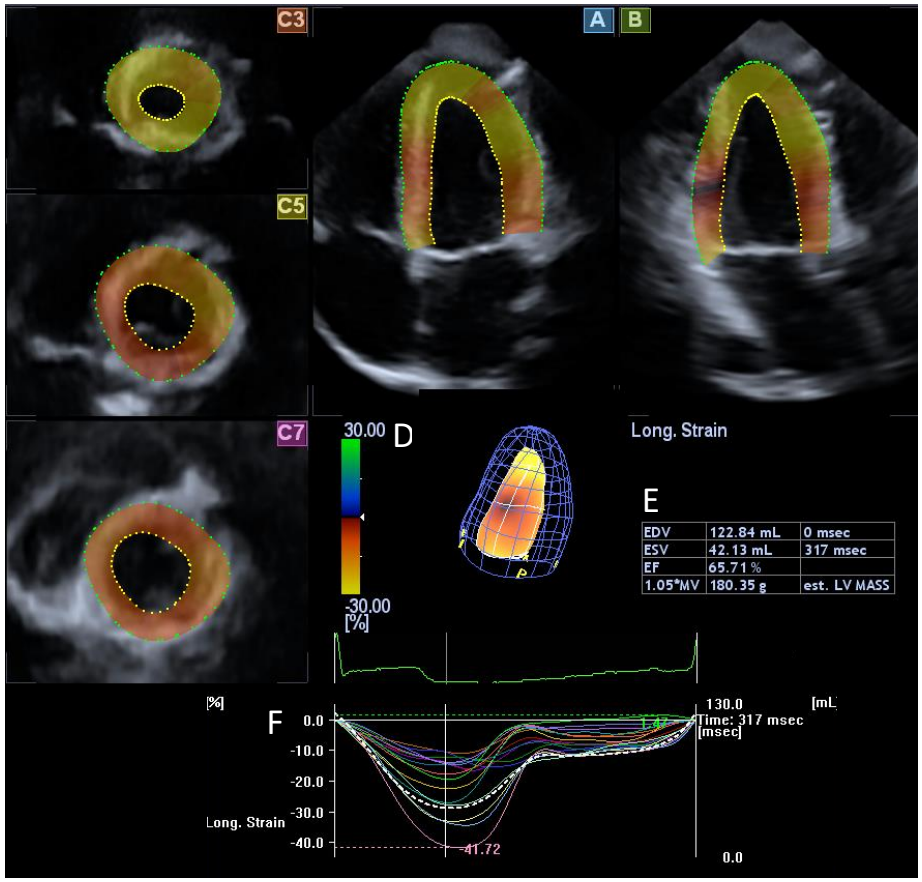

2.

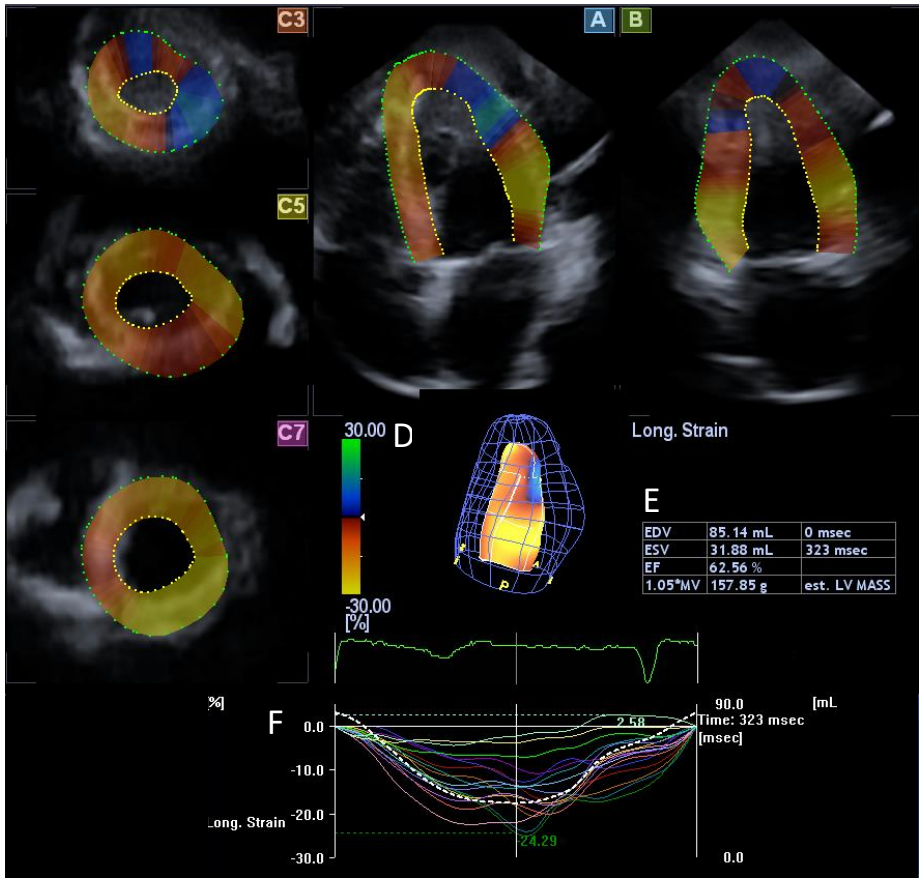

Figure 3. 3DSTE of the left ventricle of a healthy adult (panel 1) and a patient with hypereosinophilia syndrome (panel 2). From the 3D echocardiographic database collected by the special transducer, the software automatically creates sections corresponding to apical four chamber- (A) and apical two chamber views (B), and apical (C3), midventricular (C5) and basal (C7) segments in the defined cross-sectional planes. The virtual 3D model of the left ventricle (D) is automatically generated by the software after the endocardium has been detected and then the left-ventricular volumetric data, ejection fraction (E) and global / segmental strain curves (F) are calculated.

Statistical analysis. All data are reported as mean ± standard deviation. *P* values <0.05 were considered significant. Fisher's Exact test was used for categorical variables. Shapiro-Wilks test was used to test normal distribution in every dataset. Homogeneity of variance was assessed using Levene's Test for Equality of Variances. Student's t-test was used for datasets following normal distribution and Mann-Whitney-Wilcoxon test was used for datasets that were not normally distributed. RStudio was used for statistical analysis (RStudio Team (2015). RStudio: Integrated Development for R. RStudio, Inc., Boston, MA). For offline data analysis and graph creation a commercial software package was used (MATLAB 8.6, The MathWorks Inc., Natick, MA, 2015).

4. Results

4.1. Normal values of left ventricular rotational parameters in healthy adults

Patient population. To establish normal reference values of LV rotation and twist 297 healthy adults were enrolled of which 120 adults were excluded due to inferior image quality over a 6-year period (2011-2017). A volunteer was considered healthy if he or she had no currently acute disease or history of chronic disease, had no history of regular drug use and had a normal 2D echocardiogram. The remaining population was further divided into 4 subgroups based on age and gender.

Demographic and two-dimensional echocardiographic data. The healthy volunteers were divided in four different subgroups based on age: 18-29 years (mean age: 23.6 ± 2.8 years, 45 males), 30-39 years (mean age: 33.7 ± 2.8 years, 28 males), 40-49 years (mean age: 43.4 ± 3.4 years, 11 males) and 50+ years (mean age: 56.4 ± 5.3 years, 12 males). All patients underwent a complete 2D echocardiographic and Doppler assessment, the results are shown in Table 1. More than grade 1 valvular regurgitation or stenosis was excluded in study subjects.

3DSTE-derived LV volumetric data. LV ejection fraction and volumetric data derived from 3DSTE did not differ significantly between the age groups. In the age group of 18-29 years and 30-39 years 3DSTE-derived LV end-diastolic volume ($p = 0.00002$ and $p = 0.0001$, respectively) and LV end-systolic volume ($p = 0.005$ and $p = 0.04$, respectively) were significantly higher in males compared to females (Table 2).

3DSTE-derived LV rotational parameters. The results were broken down into the aforementioned 4 age groups and in each group, data were also separated based on gender (Table 2). Only the combined LV twist (average containing males and females) and the LV twist of females differed significantly between the age group of 18-29 years and 50+ years ($p = 0.02$, $p = 0.03$, respectively). In either age group, significant differences could not be detected between males and females (Figure 4.).

Left ventricular 'rigid body rotation'. LV-RBR means that the LV base and the apex rotates in the same direction, which could be either clockwise or counter-clockwise oriented. In the present study, LV RBR could be detected in 10 cases.

Table 1 Demographic and 2D echocardiographic data of enrolled healthy volunteers

	all subjects (n = 177)	males (n = 96)	females (n = 81)
Risk factors			
Age (years)	33.0 ± 12.6	33.0 ± 10.9	33.1 ± 14.4
Male gender (%)	96 (54)	96 (100)	0 (0)
Hypertension (%)	0 (0)	0 (0)	0 (0)
Diabetes mellitus (%)	0 (0)	0 (0)	0 (0)
Hyperlipidaemia (%)	0 (0)	0 (0)	0 (0)
Two-dimensional echocardiography			
LA diameter (mm)	36.6 ± 4.0	38.3 ± 3.1	34.8 ± 4.2
LV end-diastolic diameter (mm)	48.1 ± 3.7	49.2 ± 3.5	46.8 ± 3.5
LV end-diastolic volume (ml)	107.3 ± 22.8	114.1 ± 22.6	99.3 ± 20.5
LV end-systolic diameter (mm)	33.3 ± 9.7	32.7 ± 3.0	30.8 ± 3.5
LV end-systolic volume (ml)	36.5 ± 9.2	40.2 ± 8.8	32.3 ± 7.8
Interventricular septum (mm)	9.0 ± 1.6	9.6 ± 1.4	8.3 ± 1.6
LV posterior wall (mm)	9.1 ± 1.7	9.5 ± 1.4	8.6 ± 1.8
LV ejection fraction (%)	66.0 ± 5.0	64.9 ± 4.2	67.3 ± 5.5
E (cm/s)	79.9 ± 17.8	77.2 ± 16.5	83.4 ± 18.8
A (cm/s)	64.9 ± 20.3	59.4 ± 16.1	70.9 ± 22.6
E/A	1.20 ± 0.59	1.29 ± 0.52	1.10 ± 0.66

Abbreviations: LA = left atrium, LV = left ventricle, E = early transmitral flow velocity, A = late transmitral flow velocity

Feasibility of 3DSTE LV quantification. The measurements were made between 2011 and 2016, during this time period feasibility of 3DSTE analysis improved as the operators gained experience. For the overall time period the number of adequate measurements was 177 out of 297 (60% success ratio), for the last year of data gathering, the number of good quality measurements was 49 out of 60 patients (82% success ratio). This is a significant increase ($p = 0.001$).

Table 2 Three-dimensional speckle-tracking echocardiography-derived left ventricular volumetric, rotational and twist parameters of each age- and gender group

	18-29 years age group			30-39 years age group			40-49 years age group			50+ years age group		
	all subjects (n=94)	males (n=45)	females (n=49)	all subjects (n=38)	males (n=28)	females (n=10)	all subjects (n=17)	males (n=11)	females (n=6)	all subjects (n=29)	males (n=12)	females (n=17)
LV volumetric data												
EDV (ml)	86.7 ± 22.6	96.9 ± 23.9*	77.4 ± 16.9	90.4 ± 27.1	98.1 ± 27.5*	69.9 ± 10.7	78.5 ± 25.2	82.5 ± 29.3	71.8 ± 16.7	81.7 ± 19.9	89.6 ± 25.5	76.6 ± 13.8
ESV (ml)	35.8 ± 10.5	40.1 ± 11.3*	31.9 ± 8.1	37.4 ± 12.4	40.0 ± 13.3*	30.4 ± 5.5	35.4 ± 7.7	39.2 ± 5.8	29.0 ± 6.2	35.6 ± 10.9	38.9 ± 13.7	33.4 ± 8.3
EF (%)	58.9 ± 5.3	58.7 ± 5.5	59.2 ± 5.1	58.8 ± 4.8	59.6 ± 5.2	56.7 ± 2.9	56.9 ± 6.4	56.0 ± 3.7	58.4 ± 9.6	56.6 ± 7.0	57.0 ± 5.8	56.4 ± 7.8
LV rotational parameters												
LV basal rotation (deg)	-4.2 ± 2.0	-4.3 ± 2.9	-4.0 ± 1.8	-3.9 ± 1.9	-3.8 ± 1.8	-4,3 ± 2.1	-4.5 ± 2.2	-4.2 ± 2.2	-5.0 ± 2.3	-4.7 ± 2.4	-4.5 ± 2.4	- 4.9 ± 2.4
LV apical rotation (deg)	9.3 ± 3.6	9.7 ± 3.2	8.9 ± 3.9	9.3 ± 3.0	9.6 ± 3.1	8.3 ± 2.6	10.4 ± 4.2	9.7 ± 4.4	11.6 ± 3.8	10.9 ± 4.1	11.2 ± 3.4	10.7 ± 4.6
LV twist (deg)	13.5 ± 3.7	14.1 ± 3.8	13.0 ± 3.6	13.2 ± 2.6	13.4 ± 2.6	12.6 ± 2.8	14.9 ± 4.4	13.9 ± 4.0	16.6 ± 5.0	15.6 ± 4.9†	15.6 ± 3.8	15.5 ± 5.6‡
LV twist time (msec)	350 ± 84	341 ± 86	359 ± 82	336 ± 99	321 ± 61	377 ± 161	309 ± 86	294 ± 72	335 ± 107	326 ± 51	328 ± 46	324 ± 55

∗ p <0 .05 vs. females in the same age group
† p = 0.02 vs. sum LV twist in age group 18-29 years
‡ p = 0.03 vs. females' LV twist in age group 18-29 years

Abbreviations: LV = left ventricular, EDV = end- diastolic volume, ESV = end- systolic volume, EF = ejection fraction

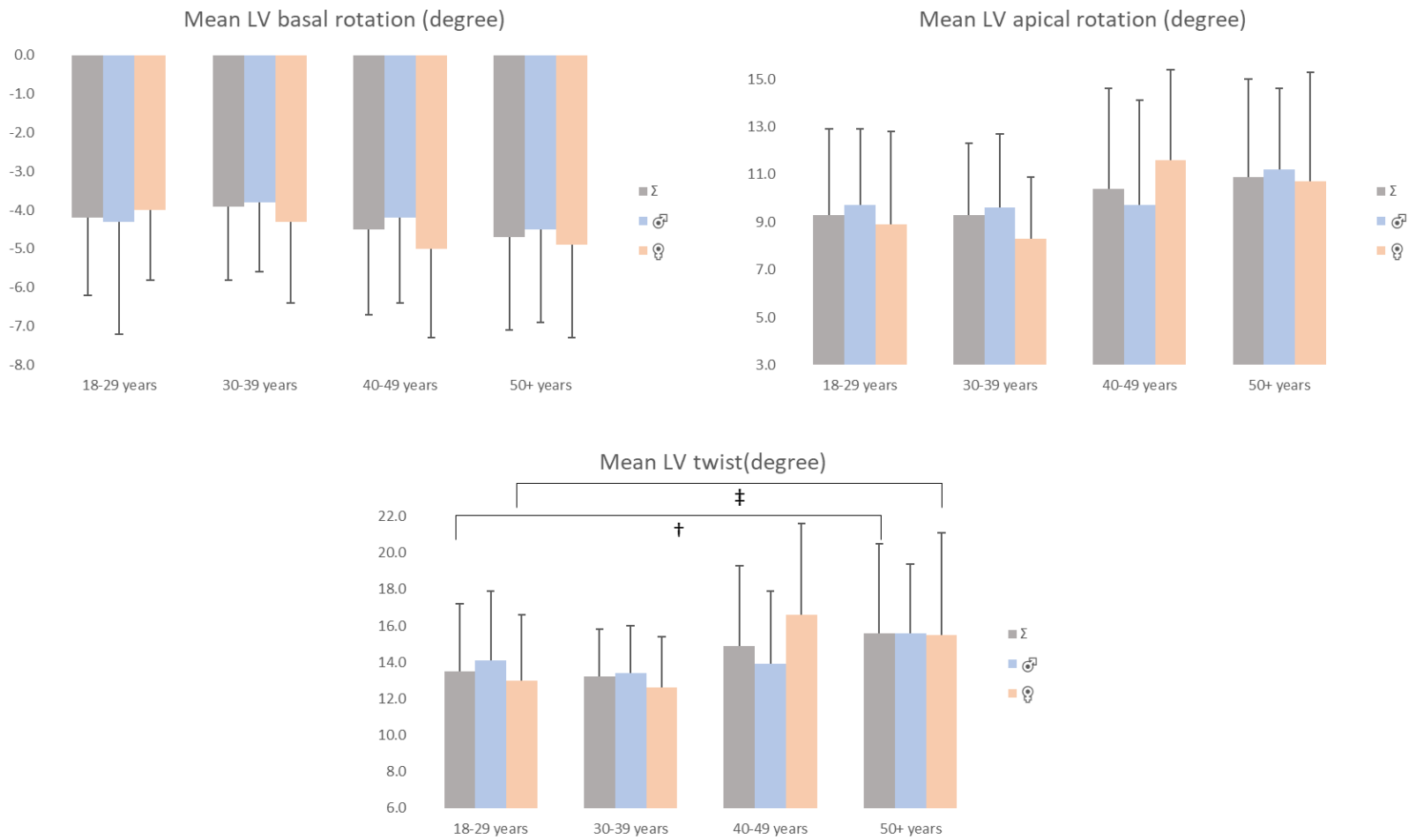

Figure 4. Mean left ventricular (LV) apical and basal rotations and LV twist across different age groups and their relation to gender are presented.
† $p < 0.05$ vs. sum LV twist in age group 18-29 years
‡ $p < 0.05$ vs. females' LV twist in age group 18-29 years

4.2. Evaluation of left ventricular rotational and twist mechanics in acromegaly

Patient population. The present study comprised 24 acromegalic patients, from which 4 patients were excluded due to insufficient image quality (mean age: 57.8 ± 13.7, 7 males). Acromegaly was diagnosed based on typical clinical features and elevated serum GH and IGF-1 levels not suppressible with oral glucose tolerant test (OGTT, 75 g) (19). Acromegaly was considered active if serum GH levels and/or serum IGF-1 levels were above the diagnostic threshold (19, 38). IGF-1 indices were also calculated in acromegaly patients, where serum IGF-1 concentration was divided by the upper limit of normal serum IGF-1 level of the same age and sex control group. All patients were sent from the Endocrinology Unit, 1st Department of Medicine at the University of Szeged. This unit is responsible for the treatment of all acromegaly patients in the region of South-East Hungary as a tertiary center. The patient population was further divided into separate subgroups based on the activity of the disease. However, due to their special LV rotational mechanics, clinical and echocardiographic data of acromegalic patients with LV RBR were managed and discussed separately.

Mean level of serum hGH was 5.50±6.75 ng/ml and mean IGF -1 serum level was 332.4±204.0 ng/ml and mean IGF-1 index was 1.45±0.91 across all acromegalic patients. Active acromegaly subgroup consisted of patients before hypophysectomy or patients who underwent surgery but had hormonally active remnant tissue or treated patients who had elevated IGF-1 levels despite long acting somatostatin analogue therapy (n=12). Mean hGH levels in this group was 4.79±4.06 ng/ml and mean IGF -1 serum level was 398±217 ng/ml and mean IGF-1 index was 1.79±0.89. Inactive acromegalic subgroup included patients who had normal serum IGF-1 and/or normal serum hGH levels or normal hGH nadir levels after OGTT during long acting somatostatin analogue, bromocriptine or pegvisomant therapy or patients who underwent successful hypophysectomy (n=8). Mean hGH levels in this group was 1.67±1.68 ng/ml and mean IGF-1 serum level was 181±113 ng/ml, mean serum levels of nadir hGH after OGGT was 1.98±2.28 ng/ml and mean IGF-1 index was 0.76±0.49. None of the acromegaly patients had chest pain or myocardial infarction before, but coronary angiography was not performed to rule out coronary artery disease.

Control group consisted of 18 age- and gender matched healthy individuals (mean age: 54.8 ± 6.9 years, 8 males).

Demographic data of acromegalic patients. Four acromegaly patients showed signs of LV RBR-like movement, these patients were delineated from the other patients. Between the

control population and the remaining 16 acromegalic patients without LV RBR-like movement there were significantly more patients with hypertension ($p<0.001$), diabetes mellitus ($p=0.04$) and hypercholesterinaemia ($p=0.002$). We got the same results between active acromegaly patients and controls ($p<0.001$, $p=0.01$, $p=0.01$, respectively). Between inactive acromegaly patients and the healthy control population only the number of patients with hypertension ($p=0.001$) and hypercholesterinaemia ($p=0.01$) were significant. There were no statistically significant differences between the active and inactive acromegaly subgroups regarding demographic data (Table 3). Data regarding the treatment of acromegaly and the number of patients who underwent hypophysectomy is also shown in Table 3.

Two-dimensional echocardiographic data We have found significant differences in LA diameter ($p=0.003$), LV end-diastolic diameter (EDD) ($p=0.001$) and LV EDV ($p<0.001$) and early filling transmitral flow velocity (E) ($p=0.03$) were found between all acromegalic patients without LV RBR and controls. Between controls and active and non-active acromegaly patient without LV RBR subgroups, LA diameter ($p=0.02$ and $p=0.02$, respectively), LV EDD ($p<0.001$ and $p=0.04$, respectively) and LV EDV ($p<0.001$ and $p=0.01$, respectively) differed significantly. No significant differences could be demonstrated between active and non-active subgroups regarding 2D echocardiographic parameters (Table 3). None of the subjects examined showed grade 3-4 mitral and tricuspid regurgitations.

Table 3. Baseline demographic and two-dimensional echocardiographic data on patients with acromegaly and controls

	Controls (n=18)	Acromegaly with LV-RBR (n=4)	Acromegaly without LV-RBR (n=16)	Active acromegaly without LV-RBR (n = 10)	Non- active acromegaly without LV-RBR (n = 6)
Risk factors					
Age (years)	54.8 ± 6.9	50.0 ± 10.6	59.7 ± 13.9	62.3 ± 12.0	55.3 ± 16.8
Male gender (%)	8 (40)	1 (25)	6 (38)	4 (40)	2 (33)
Hypertension (%)	0 (0)	1 (25)	11 (69)*	7 (70)†	4 (67)‡
Diabetes mellitus (%)	0 (0)	0 (0)	4 (25)*	4 (40)†	0 (0)
Hyperlipidaemia (%)	0 (0)	2 (50)	7 (44)*	4 (40)†	3 (50)‡
Active acromegaly	0 (0)	2 (50)	10 (63)	10 (100)	0 (0)
Treatment					
Somatostatin analogue	0 (0)	1 (25)	6 (38)	5 (50)	1 (17)
Bromoriptine	0 (0)	0 (0)	7 (44)	4 (40)	3 (50)
Pegvisomant	0 (0)	0 (0)	1 (6)	1 (10)	0 (0)
Hypophysectomy	0 (0)	3 (75)	2 (13)	2 (20)	0 (0)
Two-dimensional echocardiography					
LA diameter (mm)	37.0 ± 5.7	37.5 ± 4.3	43.2 ± 5.3*	42.8 ± 5.1†	43.7 ± 5.9‡
LV end-diastolic diameter (mm)	46.7 ± 3.8	48.7 ± 6.9	52.4 ± 5.4*	52.9 ± 4.5†	51.5 ± 6.9‡
LV end-diastolic volume (ml)	102.1± 19.3	113.5 ± 38.2	135.7 ± 28.*4	137.5 ± 24.8†	132.6 ± 35.9‡
LV end-systolic diameter (mm)	30.4 ± 2.8	30.7 ± 3.2	32.5 ± 5.2	31.7 ± 5.3	33.8 ± 5.3
LV end-systolic volume (ml)	36.0 ± 7.0	37.6 ± 9.2	44.4 ± 16.5	41.8 ± 15.8	48.6 ± 18.1
Interventricular septum (mm)	10.0 ± 1.9	9.4 ± 1.7	10.6 ± 1.8	11.0 ± 1.9	10.0 ± 1.4
LV posterior wall (mm)	10.3 ± 1.9	10.2 ± 1.8	11.2 ± 1.9	11.5 ± 1.5	10.6 ± 2.6
LV ejection fraction (%)	64.4 ± 4.1	66.2 ± 3.3	67.2 ± 8.5	69.1 ± 10.0	64.1 ± 4.1
E (cm/s)	72.5 ± 15.8	65.8 ± 11.3	61.6 ±10.0*	62.1 ± 9.4	60.8 ± 11.9
A (cm/s)	75.9 ± 17.4	86.1 ± 7.3	76.2 ± 17.2	78.7 ± 18.8	71.9 ± 14.8
E/A	1.00 ± 0.32	0.76 ± 0.11	0.84 ± 0.22	0.82 ± 0.19	0.88 ± 0.28

∗$p < 0.05$ between Acromegaly without LV-RBR group and Controls
†$p < 0.05$ between Active acromegaly group without LV-RBR and Controls
‡$p < 0.05$ between Non-active acromegaly group without LV-RBR and Controls

Abbreviations: LA=left atrial, LV=left ventricular

3DSTE–derived LV rotation and twist. Between all acromegaly patients without LV RBR–like movement and negative controls both LV basal- and apical rotation and LV twist differed significantly (p=0.0037, 0.0012, <0.001, respectively). Between active and non–active acromegaly subgroups only the time-to-peak LV twist showed significant difference (p=0.005). Between active acromegalics without LV RBR-like movement and controls, LV basal (p=0.003) and apical rotations (p=0.02) and LV twist (p=0.003) differed significantly. In case of non-active acromegaly patients without LV RBR-like movement and controls, LV apical rotation (p=0.001), LV twist (p=0.002) and time-to-peak LV twist (p=0.04) differed significantly (Table 4 and Figure 5.).

Table 4. Three-dimensional speckle-tracking echocardiography-derived parameters between various groups

	Controls (n=18)	**Acromegaly without LV-RBR (n=16)**	**Active acromegaly without LV-RBR (n=10)**	**Non-active acromegaly without LV-RBR (n=6)**
LV basal rotation deg)	-6.17 ± 2-66	-3.76± 1.73*	-3.74± 1.19†	-3.80 ± 2.52
LV apical rotation (deg)	10.81 ± 3.65	6.12 ± 4.03*	7.28 ± 3.77†	4.18 ± 4.00‡
LV twist (deg)	16.98 ± 3.88	9.88 ± 4.74*	11.03 ± 4.04†	7.98 ± 5.58‡
Time-to-peak LV basal rotation (msec)	356± 99	346 ± 144	356 ± 98	329 ± 210
Time-to-peak LV apical rotation (msec)	356 ± 79	317± 98	342 ± 75	277 ± 125
Time-to-peak LV twist (msec)	337 ± 64	321 ± 110	377 ± 78#	3229 ± 97

∗p < 0.05 between Acromegaly without LV-RBR group and Controls
†p < 0.05 between Active acromegaly without LV-RBR group and Controls
‡p < 0.05 between Non-active acromegaly without LV-RBR group and Controls
#p < 0.05 between Active acromegaly without LV-RBR group and Non-active acromegaly without LV-RBR group

Abbreviations: LV = left ventricular, EDV = end -diastolic volume, ESV = end –systolic volume, EF = ejection fraction, RBR = rigid body rotation, rot = rotation

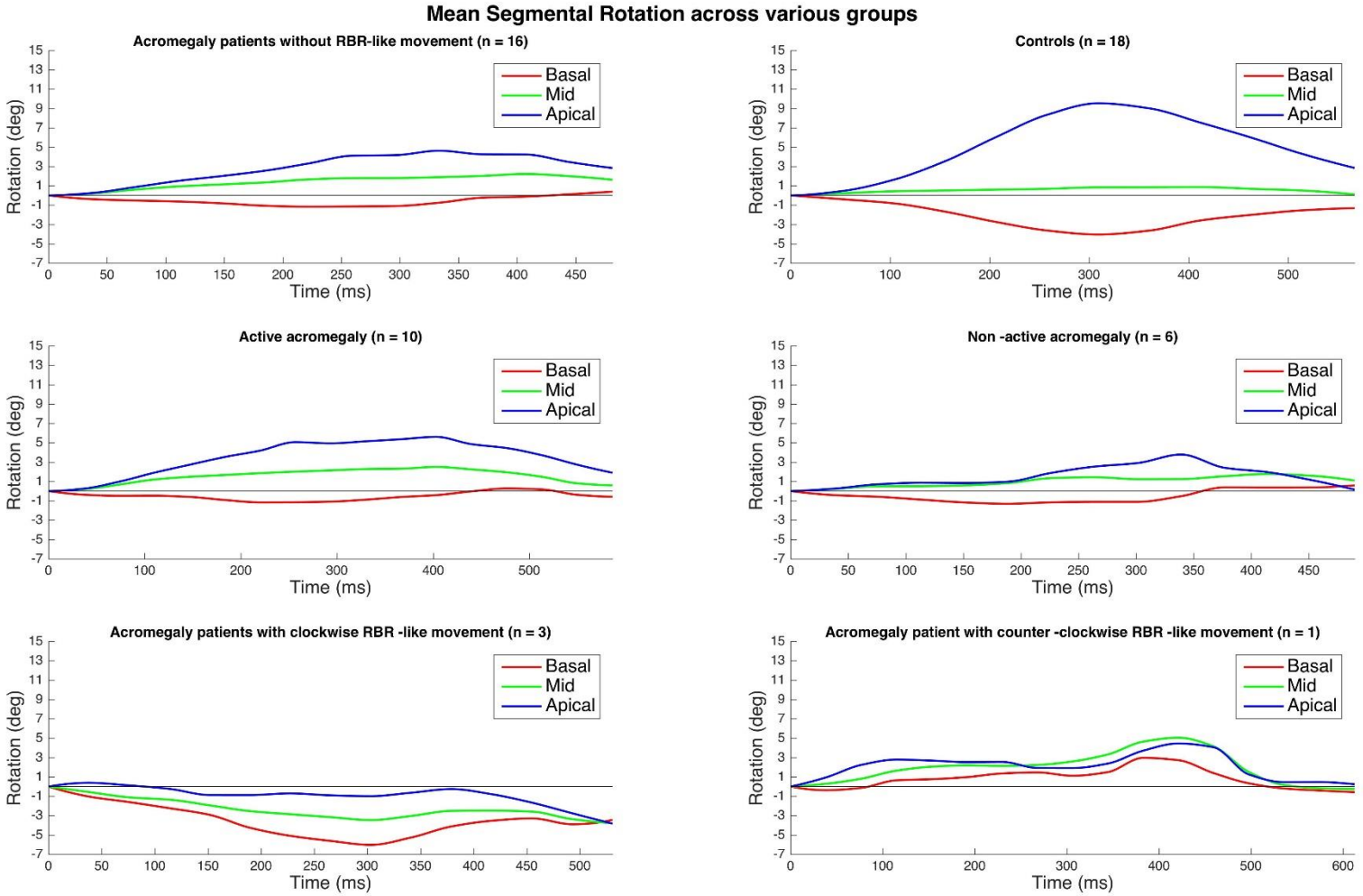

Figure 5. Mean basal, midventricular and apical LV rotations across various group are shown. **Abbreviations.** BASAL – mean LV basal rotation (red curve), MID – mean LV midventricular rotation (green curve), APICAL – mean LV apical rotation (blue curve).

Acromegaly patients with LV-RBR-like movement. As mentioned before, 4 out of 20 acromegalic patients showed LV RBR-like movements demonstrating apical and basal LV rotations in the same direction. Demographic and 2D echocardiographic data of these patients are shown in Table 3. Two out of 4 patients were active acromegaly patients, 3 had hypophysectomy in the medical history. There were no significant differences between acromegaly patients with LV RBR-like movement and other patient subgroups regarding the demographic and 2D echocardiography parameters.

Three out of 4 patients had counter-clockwise LV rotation with LV basal and apical rotations and mean apico-basal LV gradient of -5.81 ± 2.99, -0.88 ± 1.70 and 5.05 ± 2.06 degrees, respectively. Only one acromegaly patient showed clockwise LV-RBR with the same values of 1.39, 4.06 and 2.67 degrees. LV apical rotation and LV apico–basal gradient of patients with counter-clockwise LV-RBR–like movement differed significantly from LV apical rotation and LV twist of controls ($p<0.001$ and $p=0.002$, respectively). Between acromegaly patients with counter-clockwise LV-RBR–like movement and acromegaly without LV RBR-like movement group only LV apical rotation ($p=0.01$) proved to be significantly different (Table 4).

4.3. Left ventricular rotational abnormalities following successful kidney transplantation

Patient population. The present study comprised 42 KTx patients, from which 4 patients were excluded due to insufficient image quality (mean age: 46.3 ± 8.2 years, 29 males). All patients were sent from the KTx Unit at the Department of Surgery, University of Szeged minimum one year after the operation. The control group consisted of 81 age- and gender matched healthy individuals (mean age: 43.5 ± 10.8 years, 51 males).

Demographic, clinical and routine 2D echocardiographic data. The ratio of risk factors and most important medications applied in post-KTx patients are listed in Table 5. **S**ignificant differences could be demonstrated in LA diameter, LV EDD and EDV, interventricular septum, LV posterior wall thickness, LV ejection fraction and early and late filling transmitral flow velocities and in their ratio between post-KTx patients and controls (Table 5). None of the control subjects and post-KTx patients showed valvular stenosis or grade 2-4 mitral and/or tricuspid regurgitations.

Table 5. Baseline demographic and two-dimensional echocardiographic data of patients following successful kidney transplantation and of healthy controls

	Controls (n=81)	**post-KTx patients (n=42)**
Demographic data		
Age (years)	43.5 ± 10.8	46.3 ± 8.2
Male gender (%)	51 (63)	29 (69)
Hypertension (%)	0 (0)	38 (90)*
Diabetes mellitus (%)	0 (0)	8 (19)*
Hyperlipidaemia (%)	0 (0)	9 (21)*
Weight (kg)	70.3 ± 10.5	77.2 ± 12.3
Height (m)	172.4 ± 5.9	171.1 ± 8.5
Body mass index (kg/m^2)	23.5 ± 3.0	26.5 ± 3.8*
Steroid (%)	0 (0)	42 (100)*
Calcineurin inhibitor (%)	0 (0)	42 (100)*
Mycophelonate-mofetyle (%)	0 (0)	38 (90)*
β-blocker (%)	0 (0)	13 (30)*
ACE-inhibitor (%)	0 (0)	21 (50)*
Calcium-antagonist (%)	0 (0)	21 (90)*
Diuretics (%)	0 (0)	38 (90)*
Two-dimensional echocardiography		
LA diameter (mm)	37.3 ± 4.3	41.3 ± 4.7*
LV end-diastolic diameter (mm)	48.4 ± 3.9	51.9 ± 4.5*
LV end-diastolic volume (ml)	109.8 ± 24.3	132.1 ± 26.5*
LV end-systolic diameter (mm)	33.7 ± 15.2	31.1 ± 3.7
LV end-systolic volume (ml)	39.3 ± 9.4	41.0 ± 12.3
Interventricular septum (mm)	9.5 ±1.4	10.8 ±1.6*
LV posterior wall (mm)	9.6 ± 1.6	10.8 ± 1.6*
LV ejection fraction (%)	64.4 ± 3.8	67.1 ± 10.9*
E (cm/s)	74.4 ± 17.6	82.9 ± 22.9*
A (cm/s)	63.2 ± 17.1	84.9 ± 17.7*
E/A	1.23 ± 0.36	1.00 ± 0.31*

*** p<0.05 vs. Controls**

Abbreviations: ACE = angiotensin-converting enzyme, KTx = kidney transplantation, LA = left atrial, LV = left ventricular, E and A = early and late diastolic transmitral flow velocity

3DSTE–derived LV rotational and twist. Three patients following successful KTx showed near absence of LV twist called as LV RBR movement. Due to this special movement, their results were managed separately. When the remaining 35 post-KTx patients were analysed separately, reduced basal LV rotation could be demonstrated in post-KTx patients with tendentious increase in apical LV rotation resulting in an unchanged LV twist (Table 6).

Table 6 Three-dimensional speckle-tracking echocardiography-derived left ventricular volumetric and rotational parameters in patients following successful kidney transplantation and in healthy controls

	Controls (n=81)	**Post-KTx patients without LV-RBR (n=35)**
basal LV rotation (degree**)**	-4.22 ± 2.14	-3.34 ± 1.81*
apical LV rotation (degree)	9.68 ± 4.00	10.55 ± 3.67
LV twist (degree)	13.90 ± 4.33	13.89 ± 3.72
time of peak LV twist (msec)	329 ± 83	312 ± 48

***p<0.05 vs. Controls**

Abbreviations: KTx = kidney transplantation, LV = left ventricular, LV-RBR = left ventricular 'rigid body rotation'

LV-RBR. Three patients with LV RBR showed abnormally directed counterclockwise basal LV rotation (5.13 ± 3.29 degrees) and similar but normally directed counterclockwise apical rotation (14.33 ± 10.72 degrees). Therefore, real LV twist could not be measured only LV apico-basal gradient considered to be as their net difference (9.20 ± 9.04 degrees).

4.4. Differences in left ventricular rotational mechanics between lipedema and lymphedema

Patient population. The present study comprised 25 patients with stage 2 lipedema (mean age: 42.5 ± 12.2 years, body mass index (BMI): 29.9 ± 2.79 kg/m^2, all females) and 26 subjects with stage 2 bilateral leg lymphedema (mean age: 46.5 ± 11.5 years, BMI: 27.64 ± 2.6 kg/m^2, 24 females and 2 males). However mean BMI values of the two patient groups differed significantly (P=0.0049), both they belong to the moderately overweight class (25 kg/m^2<BMI<29.9 kg/m^2). All lipedema patients were diagnosed based on typical clinical features. The causes of secondary leg lymphedema were malignant melanoma treatment (n=2), gynaecological cancer treatment (n=6), bacterial cellulitis (n=2) and venous insufficiency (n=14) whereas nine lymphedema patients underwent bilateral leg lymphoscintigraphy and each patient with suspected venous disease had color duplex ultrasound examination besides clinical inspection. Each patient was sent from the Phlebolymphology Unit of the Department of Dermatology and Allergology, University of Szeged for routine cardiological examination including two-dimensional Doppler echocardiography extended with 3DSTE. Insufficient image quality for 3DSTE were detected in 3 lipedema and 4 lymphedema patients. None of the patients had known cardiovascular symptoms or diseases. Control group consisted of 54 age- and gender-matched healthy individuals (mean age: 40.7 ± 14.0 years, 3 males).

Demographic data of patients. The basic characteristics of the patients and control probands included in the study are summarized in Table 7. The groups of patients and healthy individuals matched for mean age, gender and the incidence of concomitant disorders although the size of control subject group was notably higher than those of lipedema and lymphedema cohorts.

2D echocardiographic data. Increased LA and LV dimensions could be demonstrated in lymphedema and lipedema patients without LV hypertrophy as compared to matched healthy controls. Systolic (ejection fraction) and diastolic (E/A) functions proved to be normal in both patient groups. Increased LA and LV volumetric data proved to be more pronounced in lipedema patients as compared to lymphedema cases (Table 8). None of the subjects examined showed ≥ grade 2 mitral and tricuspid regurgitations.

Table 7 Baseline demographic data on patients and controls

	Controls (n=54)	Lymphedema patients (n=26)	Lipedema patients (n=25)
Age (years)	40.7 ± 14.0	46.5 ± 11.5	42.5 ± 12.2
Male gender (%)	3 (6)	2 (8)	0 (0)
Hypertension (%)	0 (0)	1(4)	0 (0)
Diabetes mellitus (%)	0 (0)	0 (0)	0 (0)
Hyperlipidaemia (%)	0 (0)	1 (4)	0 (0)

Table 8 Two-dimensional echocardiographic data on patients and controls

	Controls (n=54)	Lymphedema patients (n=26)	Lipedema patients (n=25)
LA diameter (mm)	35.4 ± 4.1	37.7 ± 4.3*	39.9 ± 4.4*†
LV end-diastolic diameter (mm)	46.9 ± 3.6	47.8 ± 4.0	50.3 ± 3.3*†
LV end-diastolic volume (ml)	98.4 ± 21.5	109.3 ± 20.3*	121.4 ± 18.3*†
LV end-systolic diameter (mm)	36.0 ± 18.7	29.1 ± 3.5*	31.4 ± 2.7†
LV end-systolic volume (ml)	33.8 ± 8.1	33.7 ± 9.6	40.0 ± 8.2*†
Interventricular septum (mm)	8.8 ± 1.5	8.0 ± 0.9*	8.6 ± 0.9†
LV posterior wall (mm)	9.0 ± 1.7	8.2 ± 1.1*	8.6 ± 0.9
LV ejection fraction (%)	65.5 ± 4.2	69.7 ± 4.8*	67.5 ± 3.5
E (cm/s)	78.3 ± 18.1	76.8 ± 15.1	87.3 ± 18.6*†
A (cm/s)	65.5 ± 17.6	67.2 ± 14.6	78.1 ± 17.8*†
E/A	1.29 ± 0.37	1.21 ± 0.36	1.18 ± 0.40

*p<0.05 vs. Controls
†p<0.05 vs. Lymphedema patients

Abbreviations: LA = left atrial, LV = left ventricular, E and A = transmitral diastolic flow velocities

3DSTE–derived LV rotation and twist. Three lipedema and other three lymphedema patients showed significant LV rotational abnormalities, therefore their data were managed separately. Between the remaining 19 lipedema patients and negative controls only LV apical rotation and LV twist differed significantly. Similar differences between LV rotational mechanics between the remaining 19 lymphedema patients and controls could not be detected (Table 9). Moreover,

less than 1 degree LV basal rotation could be detected in 2 patients with lipedema (11%), in 2 another patients with lymphedema (11%), but in none of controls.

Table 9 Three-dimensional speckle-tracking echocardiography-derived parameters on patients and controls

	Controls (n=54)	Lymphedema patients without significant LV rotational abnormalities (n=19)	Lipedema patients without significant LV rotational abnormalities (n=19)
LV basal rotation deg)	-4.22 ± 2.17	-3.17 ± 1.50	-3.75 ± 2.01
LV apical rotation (deg)	9.61 ± 4.25	10.51 ± 4.20	6.65 ± 2.44*†
LV twist (deg)	13.83 ±4.89	13.68 ± 4.69	10.41 ± 3.24*†
Time-to-peak LV basal rotation (msec)	361 ± 105	350 ± 134	392 ± 167
Time-to-peak LV apical rotation (msec)	343 ± 105	330 ± 56	335 ± 86
Time-to-peak LV twist (msec)	354 ± 98	321 ± 70	308 ± 60

*p<0.05 vs. Controls
†p<0.05 vs. Lymphedema patients without significant LV rotational abnormalities

Abbreviations: LV = left ventricular

Lipedema and lymphedema patients with significant LV rotational abnormalities. As aforementioned, 3 out of 22 lipedema patients had significant LV rotational abnormalities. One had minimal (less than 1 degree) clockwise apical (-0.97 degree) and basal (-0.40 degree) LV rotations demonstrating almost absolute absence of LV twist in this case (-0.57 degree). Another lipedema patient had a counter-clockwise apical (14.88 degree) and similarly directed basal (6.68 degree) LV rotations resulting in an 8.20 degree counter-clockwise LV apico–basal gradient. These results suggest the near absence of LV twist with reversed basal LV rotation and compensatory apical LV hyperrotation in this case. In the third lipedema case reversed LV rotations (6.88 degree clockwise basal and 1.33 degree counterclockwise apical) could be detected. Three out of 22 lymphedema patients had counter-clockwise apical (9.19 ± 2.69 degree) and basal (3.59 ± 1.24 degree) LV rotations with mean apico-basal LV gradient of 5.59

± 2.72 degree suggesting normally directed apical, but reversed basal LV rotations in these cases (LV-RBR). Extent of apical and basal LV rotations proved to be normal in these cases. (Figure 2.)

4.5. Comparative assessment of left ventricular deformation in cardiac AL amyloidosis and hypereosinophilic syndrome

Patient population. Thirteen HES patients were enrolled in this study, of whom 2 were excluded due to inadequate image quality, and one patient fulfilled the Löffler endocarditis criteria system. The remaining 10 patients had a mean age of 60.9 ± 14.7 years (7 males). The diagnosis of HES was based on current guidelines (23). Nine of these patients had idiopathic HES, whereas in one case, acute T-lymphoma-associated HES was confirmed. No history of cardiovascular event, chronic obstructive pulmonary disease, atrial septal defect, or other malignancy was present in HES patients, and they were asymptomatic. In HES patients, the following non-cardiovascular organ involvement was reported: in one case duodenal eosinophilia, in one case eosinophilic skin symptoms, in one case lung confirmed eosinophilic cellulitis and in one case necrotizing granulomatous vasculitis. Clinical symptoms and routine echocardiographic findings suggest that all HES patients were in the early necrotic phase as thrombotic symptoms could be ruled out.

Twenty-two ALA patients participated in the study, three of whom were excluded due to inferior image quality. Accordingly, the mean age of the remaining ALA patient population was 63.4 ± 7.8 years (13 males). Cardiac involvement was diagnosed according to current guidelines (39). The location of the biopsy was in four cases the gastrointestinal tract (stomach, duodenum, colon and rectum), five cases in the kidney, seven cases in the bone marrow, three cases in the heart, two cases in the skin and one case in the salivary gland. Routine echocardiographic examination demonstrated interventricular septum and LV posterior wall thickness greater than 12 mm in all cases. In this group of patients, ALA was associated with monoclonal gammopathy of unknown origin in one case, and in the remaining 17 cases, Jamshidi biopsy confirmed multiple myeloma.

The control group consisted of 13 sex- and gender matched healthy adults with a mean age of 59.2 ± 4.3 years (5 males).

Clinical and demographic data. The ALA group had significantly more patients with hypertension and hyperlipidemia than the controls, whereas in the HES group the proportion of hypertension was significantly elevated compared to controls. There was no difference in clinical and demographic parameters between ALA and HES patient groups. No significant valvular stenosis or grade 3 valvular regurgitation could be demonstrated in any patient or control. Laboratory values for HES patients were: serum erythrocyte count: 4.01 ± 0.36 T/L, hemoglobin level: 128.0 ± 13.9 g/L, platelet count: 259.8 ± 181.2 Giga/L, hematocrit: 38.2% ± 4.2%, white blood cell count: 14.2 ± 5.9 Giga/L, ratio of eosinophils: 46.8 ± 17.2% and absolute number of eosinophils: 7.9 ± 5.1 Giga/L. The NT-proBNP level of ALA patients was 9130 ± 10121 U / l. In the ALA patient group, 3 patients had a LV ejection fraction <50%, but none of the patients exceeded the NYHA II. functional stage at the time of the study (Table 10.).

Two-dimensional echocardiographic data. Significant differences were found in LA diameter, LV end-diastolic and end-systolic diameters, interventricular septum and LV posterior wall thickness, and late transmitral flow (A) in the ALA patient group compared to controls. Similar differences between HES patients and controls could not be demonstrated. Comparison of 2D echocardiographic parameters in ALA and HES patients showed greater interventricular septum and LV posterior wall thickness in the ALA patients (Table 10.).

Left ventricular volumetric data measured by 3DSTE. There was no significant difference in ALA and HES patient groups with respect to LV-volumetric parameters measured by 3DSTE compared to the control group. Comparison of the two disease groups showed no significant difference between LV volumetric parameters (Table 10.).

Table 10. Clinical, 2D echocardiographic and 3DSTE-derived volumetric parameters of hypereosinophilia syndrome patients, light chain amyloidosis patients and healthy controls.

	Controls (n=13)	**HES patients (n=10)**	**ALA patients (n=19)**
Clinical data			
Age (years)	59.2 ± 4.3	60.9 ± 14.7	63.4 ± 7.8
Male gender (%)	5 (38)	7 (70)	13 (68)
Hypertonia (%)	0 (0)	5 (50)∗	10 (53)∗
Hyperlipidaemia (%)	0 (0)	3 (30)	8 (42)∗
Diabetes mellitus (%)	0 (0)	1 (10)	2 (11)
2D echocardiography			
LA diameter (mm)	39.3 ± 3.9	43.8 ± 6.7	44.7 ± 6.6*
LV end-diastolic diameter (mm)	49.0 ± 2.2	53.8 ± 13.0	46.4 ± 4.6*
LV end-diastolic volume (ml)	109.8 ± 15.1	114.8 ± 44.2	105.5 ± 29.7
LV end-systolic diameter (mm)	32.4 ± 2.6	37.0 ± 14.8	29.6 ± 4.7*
LV end-systolic volume (ml)	38.5 ± 6.4	45.7 ± 26.0	39.6 ± 13.9
Interventricular septum (mm)	9.6 ± 1.3	10.7 ± 1.4	13.7 ± 2.6*†
LV posterior wall (mm)	9.5 ± 1.1	10.1 ± 1.2	12.8 ± 2.1*†
E (cm/s)	68.0 ± 14.2	73.6 ± 20.7	78.01 ± 22.5
A (cm/s)	75.8 ± 20.6	75.2 ± 19.7	59.2 ± 26.6*
E/A	0.92 ± 0.20	1.02 ± 0.38	1.63 ± 0.98
LV ejection fraction (%)	64.9 ± 3.9	61.2 ± 11.5	61.1 ± 10.8
3DSTE-derived LV volumetric			
LV end-diastolic volume	77.7 ± 17.2	82.2 ± 26.6	77.8 ± 24.3
LV end-systolic volume	34.1 ± 9.6	39.3 ± 15.4	39.2 ± 19.7
LV ejection fraction (%)	56.5 ± 5.9	51.4 ± 13.9	50.5 ± 13.0

∗p<0.05 vs Controls;
†p<0.05 vs HES patients

Abbreviations: A = late diastolic transmitral flow velocity, ALA = amyloid light chain amylodisos, LA = left atrium, LV = left ventricle, E = early diastolic transmitral flow velocity, HES = hypereosinophilia syndrome

Left ventricular strain measured by 3DSTE. Compared to the control group, all basal segmental LV strains (RS, CS, LS, AS, 3DS) measured in the ALA group were significantly lower. Global and mean segmental LV LS values in ALA patients were significantly lower compared to healthy controls. Comparison of the HES patient group and the healthy controls showed a significant difference in the global LV LS and the segmental basal LV LS was also significantly lower. Comparing the values of HES and ALA patient groups, the basal LV RS and LV 3DS showed significant differences (Figure 3 and 7, Table 11).

3DSTE- derived left ventricular rotational parameters. Near absence of LV twist – the so called LV RBR - could be detected in 12 cases (63%) in the ALA patient group, while the phenomenon only occurred in one case (10%, $p < 0.05$) in the HES patient group. LV RBR was anticlockwise in both patient groups. ALA patients showing LV RBR the basal (2.31 ± 1.89 degrees) and apical LV rotation (8.44 ± 7.52 degrees) and LV apico-basal gradient were lower compared to healthy subjects (6.13 ± 7.52 degrees). In case of the only HES patient with LV RBR, the basal rotation was 1.77 degrees and the apical rotation was 14.29 degrees, corresponding to a LV apico-basal gradient of 12.52 degrees. In the remaining 7 ALA patients, basal LV rotation did not differ significantly from controls (-3.34 ± 1.58 degrees vs. -4.53 ± 2.63 degrees, $p = 0.30$), while apical LV rotation (4.81 ± 2.46 degrees vs. 10.11 ± 3.96 degrees, $p = 0.005$) and LV twist (8.15 ± 2.68 degrees vs. 14.63 ± 4.97 degree, $p = 0.005$) was significantly lower.

In the remaining 9 HES patients, LV basal rotation was not significantly different from the healthy group (-3.83 ± 2.00 degrees vs. -4.53 ± 2.63 degrees, $p = 0.50$). However, LV apical rotation (4.89 ± 2.04 degrees vs. 10.11 ± 3.96 degrees, $p = 0.002$) and LV twist (8.72 ± 2, 88 degree vs. 14.63 ± 4.97 degree, $p = 0.005$) proved to be significantly lower in HES patients compared to controls. No significant differences could be detected between ALA and HES patients.

Table 11. Values of left ventricular regional strain parameters assessed by 3DSTE in patients with hypereosinophilia syndrome, light chain amyloidosis and in healthy controls

	Controls (n=13)	**HES patients** (n=10)	**ALA patients** (n=18)
RS basal (%)	33.3 ± 9.2	35.9 ± 15.9	22.9 ± 11.8*†
RS mid (%)	30.8 ± 8.5	29.2 ± 18.3	26.0 ± 11.6
RS apex (%)	18.9 ± 10.1	15.8 ± 14.8	21.5 ± 16.3
CS basal %)	-25.8 ± 5.1	-26.3 ± 6.6	-21.2 ± 7.6*
CS mid (%)	-29.0 ± 6.7	-26.0 ± 9.3	-28.0 ± 9.5
CS apex (%)	-29.9 ± 13.9	-28.7 ± 12.7	-33.3 ± 13.1
LS basal (%)	-20.3 ± 5.2	-16.6 ± 5.3*	-14.2 ± 6.1*
LS mid %)	-13.7 ± 4.0	-12.7 ± 4.4	-11.1 ± 5.5
LS apex (%)	-15.6 ± 7.4	-15.6 ± 6.0	-17.0 ± 8.6
3DS basal (%)	35.5 ± 8.1	39.1 ± 16.0	24.6 ± 12.1*†
3DS mid (%)	31.6 ± 9.2	30.4 ± 18.2	26.6 ± 11.7
3DS apex (%)	21.1 ± 11.7	16.9 ± 15.6	24.1 ± 18.5
AS basal (%)	-40.3 ± 5.1	-37.1 ± 8.4	-31.2 ± 9.9*
AS mid (%)	-39.6 ± 8.1	-35.0 ± 11.3	-36.0 ± 11.7
AS apex (%)	-41.5 ± 17.7	-39.9 ± 15.0	-45.5 ± 16.5

∗p<0.05 vs. Controls;
†p<0.05 vs. HES patients

Abbreviations: 3DS = three-dimensional strain, ALA = amyloid light chain amyloidosis, AS = area strain, CS = circumferential strain, HES = hypereosinophilia syndrome, LS = longitudinal strain, RS = radial strain

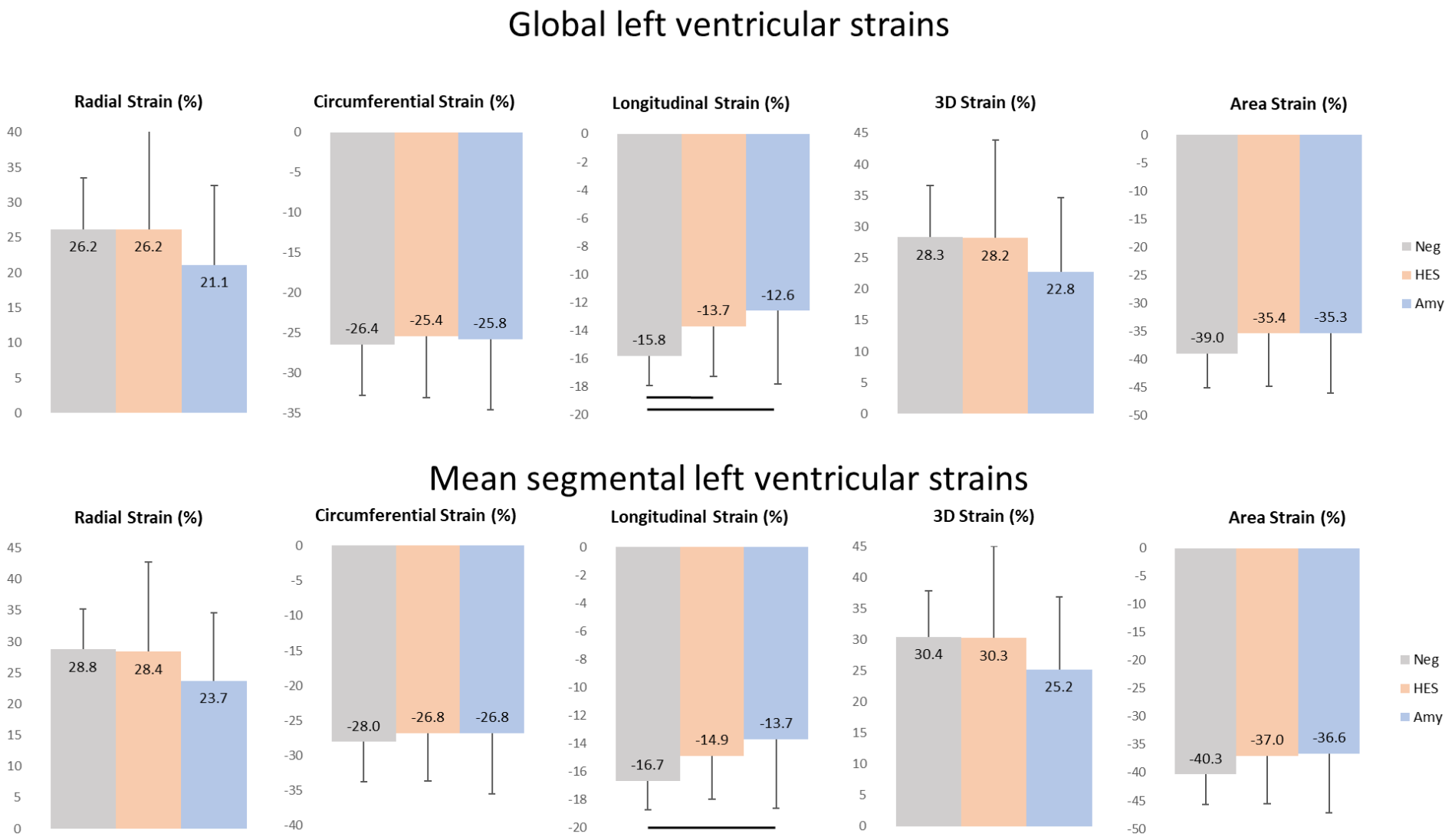

Figure 7 Values of global and mean segmental left ventricular strain parameters in the control and individual patient groups. Horizontal lines indicate significant differences between the various groups.

5. Discussion

5.1. Normal values of left ventricular rotational parameters in healthy adults

The early methods for quantifying LV rotational mechanics – such as using radiopaque markers, biplane cineangiography or sonomicrometry – were too invasive and limited methodologies (40-42). Cardiac magnetic resonance imaging (cMRI) opened a new door in this field, although this is a non-invasive, but very expensive tool, thus limiting its everyday on-demand use (43). Echocardiography on the other hand is a fast, non-invasive and widespread method in the clinical practice. Tissue Doppler imaging (TDI) and 2DSTE are both capable of LV rotation quantification. The main limitation of TDI is its angle-dependency, while 2DSTE cannot visualize the LV in real 3D and the method requires third party software, therefore guidelines are not suggesting its use in the assessment of LV rotational mechanics (44, 45). The introduction of 3DSTE seems to have solved the aforementioned issues, it is relatively fast, non-invasive and angle-independent. Also 3DSTE has been validated for quantifying LV rotation and twist against both in vitro and in vivo modalities (3, 4, 46). It is worth noting that the 3DSTE-derived LV rotational data and LV twist values seem to be lower as compared to 2DSTE, tissue Doppler imaging and tagged cMRI-derived rotational values, this is in agreement with the findings of other studies (44, 47, 48).

In the present study, it was found that the feasibility of 3DSTE grew significantly as the operators gained experience. Presented feasibility results are comparable to other groups (4, 49). It was found that LV basal and apical rotation gradually increased over time. Between the 18- 29 years- old and 30-39 years- old groups, the 2 parameters remained almost the same, however over 40 years, both LV basal and apical rotation started to rise. LV twist behaved in the same fashion reaching the level of significance between the young adulthood and the older population.

In most age groups, the degree of LV apical rotation and LV twist is non-significantly higher in males than in females. Regarding LV basal rotation, we have observed the opposite: in the age group 30- 39, 40- 49 and 50+ years, LV basal rotation is higher in females compared to males. It could be hypothesized that it is most likely due to hormonal differences between the genders. Previously, the effect of aging on LV rotational mechanics and twist were examined in a number of 2DSTE studies. In 2DSTE and 3DSTE studies, there is an agreement that regardless of gender, LV rotational and twist parameters increase with aging (47, 48, 50,

51). Notomi *et al.* reported that in infancy, the LV basal rotation is counter-clockwise and it gradually shifts over to clockwise rotation using TDI (52), in contrast to this finding, Kaku *et al.* found that in infancy the LV basal rotation is clockwise using 3DSTE (51). However, they agree that LV apical rotation is counter- clockwise and it increases along with LW twist with aging. Both papers agreed that in infancy, LV basal rotation is more dominant compared to LV apical rotation, and with aging, the emphasis shifts over to LV apical rotation (51, 52).

The underlying physiological basis of age-related increase in LV twist is not yet properly understood. Important factors such as preload, afterload and chronotropy must play a role (53-55). Lumens *et al.* suggested that the age- related LV rotational changes are due to the reduced influence of LV subendocardial fibers, therefore increasing the net LV twist (56). However, it is important to note that true experimental data is lacking.

In our study population, 10 cases with LV RBR were encountered. This phenomenon was first reported in noncompaction cardiomyopathy (NCCM) (12, 13). Our group has reported this phenomenon in a number of pathological states such as cardiac amyloidosis (57), acromegaly (58), congenital heart diseases (59-61), etc. It is not known whether this is a sign of a yet subclinical pathology or undiagnosed disease, however, to the best of our knowledge, this phenomenon has not been previously reported in the healthy population.

In recent studies it was suggested that 3DSTE seems to be a sufficient methodology for non-invasive quantification of LV rotations and twist, but clinical importance of this mechanism is poorly understood, although changes of LV rotational mechanics and twist have been reported in several pathologies (14, 57, 58). These results show that LV twisting abnormalities are associated with pathological states and they warrant further studies in this field.

Limitation section

- 3DSTE has a lower frame rate and spatial resolution compared to its 2D counterpart. Since the full volume 3D datasets are obtained through 6 RR intervals, there may be a "stitching noise" between the individual subvolumes (62). Previously a comparison study revealed that the deformation data showed some level of vendor-dependency (63).
- 3D echocardiographic systems have a tendency to underestimate LV volumetric parameters, most affected is LV-EDV, thus resulting in a seemingly lower LV-EF as compared to conventional 2D echocardiographic results (64).
- In the present paper, other chambers than the LV were not examined.

- Further imaging or other diagnostic techniques were not performed to rule out any hidden subclinical pathologies in cases with LV RBR.
- Analysing 3DSTE-derived LV strain parameters were not the goal of the present study either.

5.2 Evaluation of left ventricular rotational and twist mechanics in acromegaly

Acromegaly is a chronic, endocrine disorder with major cardiovascular comorbidity. Most prominent is hypertension, which occurs in almost 90% of acromegaly cases. The underlying pathophysiology is not clearly understood, elevated serum GH levels and consequent plasma volume expansion, increased peripheral vascular resistance and the hormone's anti-natriuretic effect may be the cause. The hypertension is not related to age or gender in acromegaly (65). The increased peripheral resistance and hypertension entails increased cardiac workload (65-67). Furthermore, acromegaly causes a specific type of cardiomyopathy, hypertrophy occurs early in the disease and prolonged elevated serum GH levels may increase prevalence up to 70-90% of all acromegaly cases. In the early stages increased Ca^{2+} sensitivity and myocardial contractibility dominates causing hyperkinetic syndrome and concentric LV hypertrophy, as the cardiac involvement progresses the cardiac hypertrophy becomes more pronounced, diastolic LV filling is decreased and pre -ejection time is prolonged. In the later stages, cardiac extracellular collagen deposition, diastolic and systolic dysfunction due to cardiac remodellation and heart failure characterises the picture. Later stages can be observed in older patients, untreated acromegaly or in cases of prolonged elevated serum GH levels (68-71). Valvular regurgitations are also frequent, mitral valve is affected in the most cases (72). Specific arrhythmias might also develop, mostly paroxysmal atrial fibrillation (73) . Lastly our group has previously demonstrated that acromegaly is associated with increased aortic stiffness (74). These changes are probably due to extracellular collagen deposition and consequent remodellation of the cardiac muscle. However, to the best of the author's knowledge this is the first study to examine LV rotational patterns and mechanics in patients with acromegaly.

In the present study 3DSTE was used for the quantification of LV basal and apical rotations and LV twist, which is considered to be the net difference of the clockwise LV basal rotation and the counter-clockwise LV apical rotation. The conventional indices of LV function have no capability to characterize LV rotational mechanics. For instance, myocardial performance index is a combined systolic-diastolic parameter featuring global LV performance,

while E/A ratio represents LV diastolic function. Due to recent developments in echocardiography, there is now the opportunity to quantify LV rotational mechanics, which have a significant role in ejection. At this moment, the number of clinical studies concerning the echocardiographic measurement of LV rotation and twist are limited, although 3DSTE has been validated for the analysis of the rotational mechanics. The advantages of 3DSTE far outweigh their disadvantages, it is fast, reproducible and measurements don't require specific skill sets.

2D echocardiography results show an enlarged heart with impaired early filling transmitral flow velocity, E/A ratio was not significantly lower compared to healthy controls, however the lowered tendency is clear. 3DSTE-derived LV basal and apical rotation and LV twist also underlines this pattern: both LV apical and basal rotation and twist proved to be diminished in acromegaly patients, furthermore LV RBR-like characteristics could be demonstrated in 4 cases. Impaired diastolic filling, high ratio of cases (20%) showing RBR–like motion of the LV and diminished LV basal and apical rotation and LV twist could be signs of acromegaly-related cardiomyopathy (75). Our findings are concordant with the above described clinical and pathophysiological features regarding the special cardiomyopathy associated with acromegaly.

Limitation section. The present study is affected by several limiting factors:

- The most important is the relatively small number of patients involved, although acromegaly is a relatively rare disorder.
- The study did not examine the effects of the drugs used with acromegaly patients. We did not take into account the elapsed time after the diagnosis and treatment and for how long the elevated serum GH levels may have been present.

5.3. Left ventricular rotational abnormalities following successful kidney transplantation

CVDs are the leading causes of morbidity and mortality in chronic kidney disease patients. KTx is the treatment modality of choice for virtually all suitable candidates with ESRD (76, 77). The leading causes of death in patients who died with a functioning allograft are CVDs as well (78), which account for almost 40 percent of all deaths in this population. Studies suggest that the survival advantage of KTx may be largely attributed to the reduction in CVDs. In a retrospective analysis of the United States Renal Data System comprising the data of more than 60,000 adult primary KTx recipients transplanted between 1995 and 2000 and more than 66,000 adult patients on the waiting list over the same time period, Meier–Kriesche *et al.* have demonstrated progressive decrease in cardiovascular death rates by renal transplant vintage for both diabetic and non-diabetic recipients of both living and deceased donor transplants (79). Diastolic dysfunction is frequently observed in ESRD, moreover, heart failure (HF) with preserved LV EF is more common in hemodialysis patients than HF with low LV-EF (80). Hassanin *et al.* demonstrated that in chronic kidney disease, although longitudinal and radial systolic functions were reduced, LV EF may remain within normal limits due to the preservation of the circumferential functions (81). KTx was found to significantly improve LV-EF and apical 4-chamber strain and to reduce LV mass index and relative wall thickness. Other variables including global longitudinal strain and diastolic dysfunction were not found to be improved significantly (82).

It is known that LV twisting mechanism is affected by several conditions and disorders, but the results are conflicting (75, 83, 84). To this point, however, there is limited information on the relationship between chronic kidney disease (CKD), KTx and LV rotational mechanics. According to Yildirim *et al.* LV rotational and twist parameters did not differ between those of predialysis and transplantation patient groups (85). In contrast, Deng *et al.* found that LV basal and apical rotations, average twist and torsion were higher following successful KTx as compared to pre-KTx results (86). Interestingly there was no significant difference between the absolute value of LV basal and apical rotations in this study.

The present study demonstrated reduced LV basal rotation and slight increase in LV apical rotation resulting in unchanged LV twist in KTx patients as compared to matched healthy controls. These results suggest a sort of remodelling of LV rotational mechanics in post-KTx patients. Moreover, significant LV rotational abnormalities (LV RBR) could also be confirmed in some KTx cases due to abnormally directed LV basal rotation. Recently these sorts of LV rotational abnormalities could be detected in high ratio of patients with NCCMP (55-100%)

(87, 88), cardiac amyloidosis (60%) (57), acromegaly (25%) (58), but reports showed similar cases with other diseases as well. Significant apico-basal gradient (overrotation of the LV apex) suggesting a compensating mechanism could also be detected in these cases similarly to what happens during stress (89). In post-KTx patients, ESRD-related consequences could explain our findings, but the effect of surgical treatment could not be excluded either (85). Further studies are warranted to confirm our findings and to compare them to renal and other functional parameters.

Limitation section. Several important limitations arose during the assessments which are listed below:

- Comparing pre- and post-transplantation data would have been the most optimal to see whether KTx has any effect on LV rotational mechanics. Unfortunately, it was not possible to make this sort of measurements and comparisons due to technical reasons. Further studies are warranted to compare pre- and post-KTx LV rotational parameters with those of matched control subjects whether KTx has any short- and long-term additive value on them.
- Coronary angiography was not performed in any of the KTx patients to exclude coronary artery disease. However, none of them had any clinical signs of angina pectoris or had previous myocardial infarction or other signs of vascular diseases.
- The effect of corresponding risk factors on the results could not be excluded.
- The present study did not aim to validate LV rotational parameters.

5.4. Left ventricular rotational mechanics differences between lipedema and lymphedema

To the best of authors' knowledge this is the first study to demonstrate that LV apical rotation and LV twist are impaired in lipedema patients, similar alterations in lymphedema patients could not be detected. Moreover, in some lipedema and lymphedema patients severe LV rotational abnormalities could be demonstrated. These alterations were not related to any demographic or echocardiographic features.

There have been no clinical studies in which cardiac alterations could be demonstrated in lipedema/lymphedema patients without overt cardiac symptoms or diseases evaluated by conventional echocardiographic methods. 3DSTE is a new non-invasive echocardiographic tool

with capability of assessing objective parameters featuring LV rotational and deformational mechanics (2, 46, 58).

Both diseases are conditions characterized by bulky lower limbs. Lipedema is associated with subcutaneous fatty oedema without relevant intersitial fluid accumulation (90), while lymphedema results from excessive retention of lymphatic fluid in the interstitial compartment. There is no clinical information on the cardiovascular adaptations to these abnormalities. In a recent study, increased aortic stiffness could be detected in lipedema (91), which is known to be associated with LV rotational mechanics (92, 93). The background of our findings is unknown however increased fluid accumulation capacity of enlarged and highly vascularized lipedematous fatty tissue and interlobular septae verified by the complicated Streten test (94) might reduce peak torsion and peak apical rotation (95). The gross proportion of mesenchymal cells in lipedematous adipose tissue may be associated with an altered composition of heart tissue including higher number of non-myocytes with nesenchymal cells that could alter left ventricular rotation (96). Moreover, subclinical epicardial fat deposition of the heart and its effect on LV rotational mechanics in lipedema patients could also not be excluded.

It can be hypothesized that subjects with significant LV rotational abnormalities are 'end-point' of the disease process but clearly it can not be stated. Further studies are warranted to confirm our findings and to assess whether LV rotational abnormalities have a diagnostic role to differentiate between lipedema from lymphedema however the present data strongly support 3DSTE measured lipedema-asociated rotational abnormalities as a novel differential diagnostic point for lymphedema beyond known parameters (94).

Limitations of the study. All aforementioned technical limiting factors of 3DSTE is also affected this study.

5.5. Comparative assessment of left ventricular deformation in cardiac AL amyloidosis and hypereosinophilic syndrome

In our study, we used the global, mean segmental, and regional LV strains and LV rotational parameters assessed by 3DSTE to compare the differences in LV deformation in HES and ALA to healthy controls. Strain analysis by 3DSTE is a validated imaging method against 2DSTE, cMRI, and TDI (2, 97-101). Recent studies have confirmed that the LV strain parameters determined during 3DSTE are somewhat lower than those determined during

2DSTE, and that there is some variation between devices offered by different manufacturers (63, 97). A significant advantage of the applied methodology compared to other modalities is its non-invasiveness, non-angle-dependency and low specific cost per study (2).

To the best of the authors' knowledge, the features of LV deformation in HES have not yet been investigated during 3DSTE. However, there are many studies in ALA patients that have been conducted on 2DSTE and 3DSTE in small numbers. A recent 3DSTE study looked at ALA patients at various Mayo stages. According to the authors, only global LV LS and LV RS differed at an early stage from healthy subjects, but at the more advanced stage of the disease, global LV CS and LV 3DS also showed significant differences (102). Our results confirmed the above, but we could only show a significant difference in the global LV LS in our patients with ALA. Nevertheless, it is clear that each strain values tend to be lower with ALA compared to both controls and HES patients. It is also evident that the strain parameters of HES patients are lower compared to the healthy population, although here only the global LV LS showed significant difference, probably due to the relatively low number of cases. Our results also suggest that LV rotational mechanics are significantly impaired in ALA patients and that LV RBR is common, this phenomenon is less common in HES patients (103).

The above-described differences in ALA are clearly explained by the deposition of light chain fibrils in the LV resulting in wall motion deficiencies and heart failure. In case of HES, theoretically, the degranulation of eosinophil cells and the consequent local inflammation and fibrosis may be behind our findings. In both cases, classical risk factors were also present in some patients, the effects of which on LV deformity cannot be excluded.

Limitation section. The results of our investigations may have been influenced by several limiting factors:

- Both HES and ALA are relatively rare diseases, so the number of cases included in our study was limited.
- Our results may have been influenced by the fact that we have not taken into account the duration of the disease and what medications were used at the time of the study.
- In the case of ALA, no correlation was found between heart failure and LV deformation.

6. Conclusions (new observations)

3DSTE seems to be a reasonably viable tool for quantification of LV rotational mechanics. According to the results of the present study it could be stated that both LV basal and apical rotation and LV twist increase with aging, regardless of gender. LV-RBR, the near absence of LV twist is also present in the normal population. Knowledge of normal reference values of 3DSTE-derived LV rotation and twist parameters could help clinicians to identify abnormal values and to recognise disease-related LV rotational abnormalities.

Acromegaly is associated with impaired LV rotational and twist mechanics as assessed by 3DSTE. LV-RBR is a frequent phenomenon in acromegaly.

KTx is associated with alterations in LV basal rotation together with unchanged LV twist suggesting the remodellation of LV twisting mechanics. The near absence of LV twist (LV-RBR) could be demonstrated in some post-KTx cases.

Lipedema is associated with impaired LV apical rotation and twist as assessed by 3DSTE, similar abnormalities in lymphedema could not be detected. In selected cases with lipedema and lymphedema severe LV rotational abnormalities could be found.

3DSTE is a suitable method for the detailed examination of LV deformation mechanics in HES and ALA patient groups. Significant deformation differences were observed in both patient groups, these changes are more pronounced in the ALA patient group.

7. References

1. Nemes A, Forster T. [Recent echocardiographic examination of the left ventricle - from M-mode to 3D speckle-tracking imaging]. Orv Hetil. 2015;156(43):1723-40.
2. Nemes A, Kalapos A, Domsik P, Forster T. [Three-dimensional speckle-tracking echocardiography -- a further step in non-invasive three-dimensional cardiac imaging]. Orv Hetil. 2012;153(40):1570-7.
3. Ashraf M, Myronenko A, Nguyen T, Inage A, Smith W, Lowe RI, et al. Defining left ventricular apex-to-base twist mechanics computed from high-resolution 3D echocardiography: validation against sonomicrometry. JACC Cardiovasc Imaging. 2010;3(3):227-34.
4. Andrade J, Cortez LD, Campos O, Arruda AL, Pinheiro J, Vulcanis L, et al. Left ventricular twist: comparison between two- and three-dimensional speckle-tracking echocardiography in healthy volunteers. Eur J Echocardiogr. 2011;12(1):76-9.
5. Keele KD. Leonardo da Vinci, and the movement of the heart. Proc R Soc Med. 1951;44(3):209-13.
6. Sengupta PP, Tajik AJ, Chandrasekaran K, Khandheria BK. Twist mechanics of the left ventricle: principles and application. JACC Cardiovasc Imaging. 2008;1(3):366-76.
7. Armour JA, Randall WC. Structural basis for cardiac function. Am J Physiol. 1970;218(6):1517-23.
8. Greenbaum RA, Ho SY, Gibson DG, Becker AE, Anderson RH. Left ventricular fibre architecture in man. Br Heart J. 1981;45(3):248-63.
9. Sengupta PP, Korinek J, Belohlavek M, Narula J, Vannan MA, Jahangir A, et al. Left ventricular structure and function: basic science for cardiac imaging. J Am Coll Cardiol. 2006;48(10):1988-2001.
10. Bloechlinger S, Grander W, Bryner J, Dunser MW. Left ventricular rotation: a neglected aspect of the cardiac cycle. Intensive Care Med. 2011;37(1):156-63.
11. Nakatani S. Left ventricular rotation and twist: why should we learn? J Cardiovasc Ultrasound. 2011;19(1):1-6.
12. van Dalen BM, Caliskan K, Soliman OI, Nemes A, Vletter WB, Ten Cate FJ, et al. Left ventricular solid body rotation in non-compaction cardiomyopathy: a potential new objective and quantitative functional diagnostic criterion? Eur J Heart Fail. 2008;10(11):1088-93.
13. Nemes A, Kalapos A, Domsik P, Forster T. Identification of left ventricular "rigid body rotation" by three-dimensional speckle-tracking echocardiography in a patient with noncompaction of the left ventricle: a case from the MAGYAR-Path Study. Echocardiography. 2012;29(9):E237-40.
14. Stohr EJ, Shave RE, Baggish AL, Weiner RB. Left ventricular twist mechanics in the context of normal physiology and cardiovascular disease: a review of studies using speckle tracking echocardiography. Am J Physiol Heart Circ Physiol. 2016;311(3):H633-44.
15. Sanno N, Teramoto A, Osamura RY, Horvath E, Kovacs K, Lloyd RV, et al. Pathology of pituitary tumors. Neurosurg Clin N Am. 2003;14(1):25-39, vi.
16. Colao A, Ferone D, Marzullo P, Lombardi G. Systemic complications of acromegaly: epidemiology, pathogenesis, and management. Endocr Rev. 2004;25(1):102-52.
17. Clayton RN. Cardiovascular function in acromegaly. Endocr Rev. 2003;24(3):272-7.
18. Ramos-Levi AM, Marazuela M. Cardiovascular comorbidities in acromegaly: an update on their diagnosis and management. Endocrine. 2017;55(2):346-59.
19. Melmed S. Medical progress: Acromegaly. N Engl J Med. 2006;355(24):2558-73.
20. Rao NN, Coates PT. Cardiovascular Disease After Kidney Transplant. Semin Nephrol. 2018;38(3):291-7.
21. Lee BB, Antignani PL, Baroncelli TA, Boccardo FM, Brorson H, Campisi C, et al. IUA-ISVI consensus for diagnosis guideline of chronic lymphedema of the limbs. Int Angiol. 2015;34(4):311-32.
22. Lee BB, Andrade M, Antignani PL, Boccardo F, Bunke N, Campisi C, et al. Diagnosis and treatment of primary lymphedema. Consensus document of the International Union of Phlebology (IUP)-2013. Int Angiol. 2013;32(6):541-74.
23. Gotlib J. World Health Organization-defined eosinophilic disorders: 2017 update on diagnosis, risk stratification, and management. Am J Hematol. 2017;92(11):1243-59.

24. Klion A. Hypereosinophilic syndrome: approach to treatment in the era of precision medicine. Hematology Am Soc Hematol Educ Program. 2018;2018(1):326-31.
25. Kim NK, Kim CY, Kim JH, Jang SY, Bae MH, Lee JH, et al. A Hypereosinophilic Syndrome with Cardiac Involvement from Thrombotic Stage to Fibrotic Stage. J Cardiovasc Ultrasound. 2015;23(2):100-2.
26. Mankad R, Bonnichsen C, Mankad S. Hypereosinophilic syndrome: cardiac diagnosis and management. Heart. 2016;102(2):100-6.
27. Kleinfeldt T, Nienaber CA, Kische S, Akin I, Turan RG, Korber T, et al. Cardiac manifestation of the hypereosinophilic syndrome: new insights. Clin Res Cardiol. 2010;99(7):419-27.
28. Nemes A, Marton I, Domsik P, Kalapos A, Posfai E, Modok S, et al. The right atrium in idiopathic hypereosinophilic syndrome : Insights from the 3D speckle tracking echocardiographic MAGYAR-Path Study. Herz. 2017.
29. Nemes A, Marton I, Domsik P, Kalapos A, Posfai E, Modok S, et al. Characterization of left atrial dysfunction in hypereosinophilic syndrome - Insights from the Motion analysis of the heart and great vessels by three-dimensional speckle tracking echocardiography in pathological cases (MAGYAR-Path) Study. Rev Port Cardiol. 2016;35(5):277-83.
30. Sipe JD, Benson MD, Buxbaum JN, Ikeda SI, Merlini G, Saraiva MJ. Amyloid fibril proteins and amyloidosis: chemical identification and clinical classification International Society of Amyloidosis 2016 Nomenclature Guidelines. 2016;23(4):209-13.
31. Esplin BL, Gertz MA. Current trends in diagnosis and management of cardiac amyloidosis. Curr Probl Cardiol. 2013;38(2):53-96.
32. Tan SY, Pepys MB. Amyloidosis. Histopathology. 1994;25(5):403-14.
33. Merlini G. CyBorD: stellar response rates in AL amyloidosis. Blood. 2012;119(19):4343-5.
34. Merlini G, Lousada I, Ando Y, Dispenzieri A, Gertz MA, Grogan M, et al. Rationale, application and clinical qualification for NT-proBNP as a surrogate end point in pivotal clinical trials in patients with AL amyloidosis. Leukemia. 2016;30(10):1979-86.
35. Kumar S, Dispenzieri A, Lacy MQ, Hayman SR, Buadi FK, Colby C, et al. Revised prognostic staging system for light chain amyloidosis incorporating cardiac biomarkers and serum free light chain measurements. J Clin Oncol. 2012;30(9):989-95.
36. Cheng ZW, Tian Z, Kang L, Chen TB, Fang LG, Cheng KA, et al. [Electrocardiographic and echocardiographic features of patients with primary cardiac amyloidosis]. Zhonghua Xin Xue Guan Bing Za Zhi. 2010;38(7):606-9.
37. Lang RM, Badano LP, Mor-Avi V, Afilalo J, Armstrong A, Ernande L, et al. Recommendations for cardiac chamber quantification by echocardiography in adults: an update from the American Society of Echocardiography and the European Association of Cardiovascular Imaging. Eur Heart J Cardiovasc Imaging. 2015;16(3):233-70.
38. Vilar L, Vilar CF, Lyra R, Lyra R, Naves LA. Acromegaly: clinical features at diagnosis. Pituitary. 2016.
39. Falk RH, Alexander KM, Liao R, Dorbala S. AL (Light-Chain) Cardiac Amyloidosis: A Review of Diagnosis and Therapy. J Am Coll Cardiol. 2016;68(12):1323-41.
40. Arts T, Hunter WC, Douglas AS, Muijtjens AM, Corsel JW, Reneman RS. Macroscopic three-dimensional motion patterns of the left ventricle. Adv Exp Med Biol. 1993;346:383-92.
41. Hansen DE, Daughters GT, 2nd, Alderman EL, Ingels NB, Jr., Miller DC. Torsional deformation of the left ventricular midwall in human hearts with intramyocardial markers: regional heterogeneity and sensitivity to the inotropic effects of abrupt rate changes. Circ Res. 1988;62(5):941-52.
42. Gorman JH, 3rd, Gupta KB, Streicher JT, Gorman RC, Jackson BM, Ratcliffe MB, et al. Dynamic three-dimensional imaging of the mitral valve and left ventricle by rapid sonomicrometry array localization. J Thorac Cardiovasc Surg. 1996;112(3):712-26.
43. Buchalter MB, Weiss JL, Rogers WJ, Zerhouni EA, Weisfeldt ML, Beyar R, et al. Noninvasive quantification of left ventricular rotational deformation in normal humans using magnetic resonance imaging myocardial tagging. Circulation. 1990;81(4):1236-44.
44. Notomi Y, Setser RM, Shiota T, Martin-Miklovic MG, Weaver JA, Popovic ZB, et al. Assessment of left ventricular torsional deformation by Doppler tissue imaging: validation study with tagged magnetic resonance imaging. Circulation. 2005;111(9):1141-7.

45. Helle-Valle T, Crosby J, Edvardsen T, Lyseggen E, Amundsen BH, Smith HJ, et al. New noninvasive method for assessment of left ventricular rotation: speckle tracking echocardiography. Circulation. 2005;112(20):3149-56.
46. Zhou Z, Ashraf M, Hu D, Dai X, Xu Y, Kenny B, et al. Three-dimensional speckle-tracking imaging for left ventricular rotation measurement: an in vitro validation study. J Ultrasound Med. 2010;29(6):903-9.
47. Kocabay G, Muraru D, Peluso D, Cucchini U, Mihaila S, Padayattil-Jose S, et al. Normal left ventricular mechanics by two-dimensional speckle-tracking echocardiography. Reference values in healthy adults. Rev Esp Cardiol (Engl Ed). 2014;67(8):651-8.
48. van Dalen BM, Soliman OI, Vletter WB, ten Cate FJ, Geleijnse ML. Age-related changes in the biomechanics of left ventricular twist measured by speckle tracking echocardiography. Am J Physiol Heart Circ Physiol. 2008;295(4):H1705-11.
49. Muraru D, Niero A, Rodriguez-Zanella H, Cherata D, Badano L. Three-dimensional speckle-tracking echocardiography: benefits and limitations of integrating myocardial mechanics with three-dimensional imaging. Cardiovasc Diagn Ther. 2018;8(1):101-17.
50. Tavakoli V, Sahba N. Assessment of age-related changes in left ventricular twist by 3-dimensional speckle-tracking echocardiography. J Ultrasound Med. 2013;32(8):1435-41.
51. Kaku K, Takeuchi M, Tsang W, Takigiku K, Yasukochi S, Patel AR, et al. Age-related normal range of left ventricular strain and torsion using three-dimensional speckle-tracking echocardiography. J Am Soc Echocardiogr. 2014;27(1):55-64.
52. Notomi Y, Srinath G, Shiota T, Martin-Miklovic MG, Beachler L, Howell K, et al. Maturational and adaptive modulation of left ventricular torsional biomechanics: Doppler tissue imaging observation from infancy to adulthood. Circulation. 2006;113(21):2534-41.
53. Fujimoto N, Hastings JL, Bhella PS, Shibata S, Gandhi NK, Carrick-Ranson G, et al. Effect of ageing on left ventricular compliance and distensibility in healthy sedentary humans. J Physiol. 2012;590(8):1871-80.
54. Lakatta EG, Levy D. Arterial and cardiac aging: major shareholders in cardiovascular disease enterprises: Part II: the aging heart in health: links to heart disease. Circulation. 2003;107(2):346-54.
55. McEniery CM, Yasmin, Hall IR, Qasem A, Wilkinson IB, Cockcroft JR, et al. Normal vascular aging: differential effects on wave reflection and aortic pulse wave velocity: the Anglo-Cardiff Collaborative Trial (ACCT). J Am Coll Cardiol. 2005;46(9):1753-60.
56. Lumens J, Delhaas T, Arts T, Cowan BR, Young AA. Impaired subendocardial contractile myofiber function in asymptomatic aged humans, as detected using MRI. Am J Physiol Heart Circ Physiol. 2006;291(4):H1573-9.
57. Nemes A, Foldeak D, Domsik P, Kalapos A, Sepp R, Borbenyi Z, et al. Different patterns of left ventricular rotational mechanics in cardiac amyloidosis-results from the three-dimensional speckle-tracking echocardiographic MAGYAR-Path Study. Quant Imaging Med Surg. 2015;5(6):853-7.
58. Kormanyos A, Domsik P, Kalapos A, Orosz A, Lengyel C, Valkusz Z, et al. Left ventricular twist is impaired in acromegaly: Insights from the three-dimensional speckle tracking echocardiographic MAGYAR-Path Study. J Clin Ultrasound. 2018;46(2):122-8.
59. Nemes A, Havasi K, Domsik P, Kalapos A, Forster T. Left Ventricular Rigid Body Rotation in Ebstein's Anomaly from the MAGYAR-Path Study. Arq Bras Cardiol. 2016;106(6):544-5.
60. Nemes A, Havasi K, Domsik P, Kalapos A, Forster T. Can univentricular heart be associated with "rigid body rotation"? A case from the threedimensional speckle-tracking echocardiographic MAGYAR-path study. Hellenic J Cardiol. 2015;56(2):186-8.
61. Nemes A, Havasi K, Forster T. "Rigid body rotation" of the left ventricle in hypoplastic right-heart syndrome: a case from the three-dimensional speckle-tracking echocardiographic MAGYAR-Path Study. Cardiol Young. 2015;25(4):768-72.
62. Seo Y, Ishizu T, Aonuma K. Current status of 3-dimensional speckle tracking echocardiography: a review from our experiences. J Cardiovasc Ultrasound. 2014;22(2):49-57.
63. Gayat E, Ahmad H, Weinert L, Lang RM, Mor-Avi V. Reproducibility and inter-vendor variability of left ventricular deformation measurements by three-dimensional speckle-tracking echocardiography. J Am Soc Echocardiogr. 2011;24(8):878-85.

64. Driessen MM, Kort E, Cramer MJ, Doevendans PA, Angevaare MJ, Leiner T, et al. Assessment of LV ejection fraction using real-time 3D echocardiography in daily practice: direct comparison of the volumetric and speckle tracking methodologies to CMR. Neth Heart J. 2014;22(9):383-90.
65. Vitale G, Pivonello R, Auriemma RS, Guerra E, Milone F, Savastano S, et al. Hypertension in acromegaly and in the normal population: prevalence and determinants. Clin Endocrinol (Oxf). 2005;63(4):470-6.
66. Bondanelli M, Ambrosio MR, degli Uberti EC. Pathogenesis and prevalence of hypertension in acromegaly. Pituitary. 2001;4(4):239-49.
67. Brevetti G, Marzullo P, Silvestro A, Pivonello R, Oliva G, di Somma C, et al. Early vascular alterations in acromegaly. J Clin Endocrinol Metab. 2002;87(7):3174-9.
68. Colao A, Marzullo P, Di Somma C, Lombardi G. Growth hormone and the heart. Clin Endocrinol (Oxf). 2001;54(2):137-54.
69. Bogazzi F, Lombardi M, Strata E, Aquaro G, Di Bello V, Cosci C, et al. High prevalence of cardiac hypertophy without detectable signs of fibrosis in patients with untreated active acromegaly: an in vivo study using magnetic resonance imaging. Clin Endocrinol (Oxf). 2008;68(3):361-8.
70. Sacca L, Napoli R, Cittadini A. Growth hormone, acromegaly, and heart failure: an intricate triangulation. Clin Endocrinol (Oxf). 2003;59(6):660-71.
71. Powlson AS, Gurnell M. Cardiovascular Disease and Sleep-Disordered Breathing in Acromegaly. Neuroendocrinology. 2016;103(1):75-85.
72. Pereira AM, van Thiel SW, Lindner JR, Roelfsema F, van der Wall EE, Morreau H, et al. Increased prevalence of regurgitant valvular heart disease in acromegaly. J Clin Endocrinol Metab. 2004;89(1):71-5.
73. Kahaly G, Olshausen KV, Mohr-Kahaly S, Erbel R, Boor S, Beyer J, et al. Arrhythmia profile in acromegaly. Eur Heart J. 1992;13(1):51-6.
74. Nemes A, Gavaller H, Csajbok E, Julesz J, Forster T, Csanady M. Aortic stiffness is increased in acromegaly--a transthoracic echocardiographic study. Int J Cardiol. 2008;124(1):121-3.
75. Phillips AA, Cote AT, Bredin SS, Warburton DE. Heart disease and left ventricular rotation - a systematic review and quantitative summary. BMC Cardiovasc Disord. 2012;12:46.
76. Kasiske BL, Chakkera HA, Roel J. Explained and unexplained ischemic heart disease risk after renal transplantation. J Am Soc Nephrol. 2000;11(9):1735-43.
77. Sarnak MJ, Levey AS, Schoolwerth AC, Coresh J, Culleton B, Hamm LL, et al. Kidney disease as a risk factor for development of cardiovascular disease: a statement from the American Heart Association Councils on Kidney in Cardiovascular Disease, High Blood Pressure Research, Clinical Cardiology, and Epidemiology and Prevention. Circulation. 2003;108(17):2154-69.
78. Ojo AO. Cardiovascular complications after renal transplantation and their prevention. Transplantation. 2006;82(5):603-11.
79. Meier-Kriesche HU, Schold JD, Kaplan B. Long-term renal allograft survival: have we made significant progress or is it time to rethink our analytic and therapeutic strategies? Am J Transplant. 2004;4(8):1289-95.
80. Ogawa T, Koeda M, Nitta K. Left Ventricular Diastolic Dysfunction in End-Stage Kidney Disease: Pathogenesis, Diagnosis, and Treatment. Ther Apher Dial. 2015;19(5):427-35.
81. Hassanin N, Alkemary A. Early Detection of Subclinical Uremic Cardiomyopathy Using Two-Dimensional Speckle Tracking Echocardiography. Echocardiography. 2016;33(4):527-36.
82. Hamidi S, Kojuri J, Attar A, Roozbeh J, Moaref A, Nikoo MH. The effect of kidney transplantation on speckled tracking echocardiography findings in patients on hemodialysis. J Cardiovasc Thorac Res. 2018;10(2):90-4.
83. Nemes A, Dezsi L, Domsik P, Kalapos A, Forster T, Vecsei L. Left ventricular deformation abnormalities in a patient with calpainopathy-a case from the three-dimensional speckle-tracking echocardiographic MAGYAR-Path Study. Quant Imaging Med Surg. 2017;7(6):685-90.
84. Nemes A, Katona M, Domsik P, Kalapos A, Forster T. Different patterns of left ventricular "rigid body rotation" in 8-year-old twins with anamnestic twin-to-twin transfusion syndrome (from the MAGYAR-Twin Study). Quant Imaging Med Surg. 2017;7(1):140-1.
85. Yildirim U, Gulel O, Eksi A, Dilek M, Demircan S, Sahin M. The effect of different treatment strategies on left ventricular myocardial deformation parameters in patients with chronic renal failure. Int J Cardiovasc Imaging. 2018;34(11):1731-9.

86. Deng Y, Pandit A, Heilman RL, Chakkera HA, Mazur MJ, Mookadam F. Left ventricular torsion changes post kidney transplantation. J Cardiovasc Ultrasound. 2013;21(4):171-6.
87. Peters F, Khandheria BK, Libhaber E, Maharaj N, Dos Santos C, Matioda H, et al. Left ventricular twist in left ventricular noncompaction. Eur Heart J Cardiovasc Imaging. 2014;15(1):48-55.
88. Kalapos A, Domsik P, Forster T, Nemes A. [Comparative evaluation of left ventricular function by two-dimensional echocardiography and three-dimensional speckle-tracking echocardiography in noncompaction cardiomyopathy. Results from the MAGYAR-Path Study]. Orv Hetil. 2013;154(34):1352-9.
89. Nemes A, Szanto G, Domsik P, Kormanyos A, Kalapos A, Ambrus N, et al. Change of left ventricular "rigid body rotation" during dipyridamole-induced vasodilation: A case from the three-dimensional speckle tracking echocardiographic MAGYAR-Stress Study. J Clin Ultrasound. 2018;46(2):152-6.
90. Szel E, Kemeny L, Groma G, Szolnoky G. Pathophysiological dilemmas of lipedema. Med Hypotheses. 2014;83(5):599-606.
91. Szolnoky G, Nemes A, Gavaller H, Forster T, Kemeny L. Lipedema is associated with increased aortic stiffness. Lymphology. 2012;45(2):71-9.
92. Nemes A, Kalapos A, Domsik P, Lengyel C, Orosz A, Forster T. Correlations between echocardiographic aortic elastic properties and left ventricular rotation and twist--insights from the three-dimensional speckle-tracking echocardiographic MAGYAR-Healthy Study. Clin Physiol Funct Imaging. 2013;33(5):381-5.
93. Sulemane S, Panoulas VF, Konstantinou K, Bratsas A, Tam FW, Brown EA, et al. Left ventricular twist mechanics and its relation with aortic stiffness in chronic kidney disease patients without overt cardiovascular disease. Cardiovasc Ultrasound. 2016;14:10.
94. Forner-Cordero I, Szolnoky G, Forner-Cordero A, Kemeny L. Lipedema: an overview of its clinical manifestations, diagnosis and treatment of the disproportional fatty deposition syndrome - systematic review. Clin Obes. 2012;2(3-4):86-95.
95. Bloechlinger S, Berger D, Bryner J, Wiegand J, Dunser MW, Takala J. Left ventricular torsion abnormalities in septic shock and corrective effect of volume loading: a pilot study. Can J Cardiol. 2013;29(12):1665-71.
96. Varga I, Kyselovic J, Galfiova P, Danisovic L. The Non-cardiomyocyte Cells of the Heart. Their Possible Roles in Exercise-Induced Cardiac Regeneration and Remodeling. Adv Exp Med Biol. 2017;999:117-36.
97. Saito K, Okura H, Watanabe N, Hayashida A, Obase K, Imai K, et al. Comprehensive evaluation of left ventricular strain using speckle tracking echocardiography in normal adults: comparison of three-dimensional and two-dimensional approaches. J Am Soc Echocardiogr. 2009;22(9):1025-30.
98. Ammar KA, Paterick TE, Khandheria BK, Jan MF, Kramer C, Umland MM, et al. Myocardial mechanics: understanding and applying three-dimensional speckle tracking echocardiography in clinical practice. Echocardiography. 2012;29(7):861-72.
99. Nesser HJ, Mor-Avi V, Gorissen W, Weinert L, Steringer-Mascherbauer R, Niel J, et al. Quantification of left ventricular volumes using three-dimensional echocardiographic speckle tracking: comparison with MRI. Eur Heart J. 2009;30(13):1565-73.
100. Kleijn SA, Brouwer WP, Aly MF, Russel IK, de Roest GJ, Beek AM, et al. Comparison between three-dimensional speckle-tracking echocardiography and cardiac magnetic resonance imaging for quantification of left ventricular volumes and function. Eur Heart J Cardiovasc Imaging. 2012;13(10):834-9.
101. Kleijn SA, Aly MF, Terwee CB, van Rossum AC, Kamp O. Reliability of left ventricular volumes and function measurements using three-dimensional speckle tracking echocardiography. Eur Heart J Cardiovasc Imaging. 2012;13(2):159-68.
102. Pradel S, Magne J, Jaccard A, Fadel BM, Boulogne C, Salemi VMC, et al. Left ventricular assessment in patients with systemic light chain amyloidosis: a 3-dimensional speckle tracking transthoracic echocardiographic study. Int J Cardiovasc Imaging. 2019;35(5):845-54.
103. Nemes A, Kormányos Á, Marton I, Domsik P, Kalapos A, Ambrus N, Borbényi Z. Left ventricular rotational mechanics in hypereosinophilic syndrome – Analysis from the three-dimensional speckle-tracking echocardiographic MAGYAR-Path Study. Echocardiography. 2019;in press.

Acknowledgements

All studies reported in this work were carried out at the 2nd Department of Medicine and Cardiology Center, Medical Faculty, Albert Szent-Györgyi Clinical Center, University of Szeged, Hungary.

First of all, I would like to thank my supervisor and scientific mentor, Prof. Dr. Attila Nemes, for his continuous support throughout the years and for his help with my work, without him this dissertation would not have been possible.

I would also like to express my heartfelt gratitude towards my mentor, Dr. Kálmán Havasi, for whom I owe my professional development. Without his everyday support and care I would not be the doctor that I am today.

I would like to thank very much also Prof. Dr. Tamás Forster, the former head of the 2nd Department of Medicine and Cardiology Center, who supported me in my work.

I would like to thank all co-authors, especially Dr. Péter Domsik, Dr. Anita Kalapos, Dr. Nándor Gyenes, Dr. Nóra Ambrus, Dr. Dóra Földeák, Dr. Imelda Marton, Dr. Szabolcs Modok, Dr. Attila Trencsányi, Dr. Andrea Orosz, Dr. Zsuzsanna Valkusz, Dr. Bernadett Borda, Dr. Győző Szolnoky, Prof. Dr. György Lázár, Prof. Dr. Zita Borbényi, Prof. Dr. Lajos Kemény and Prof. Dr. Csaba Lengyel

I thank all my colleagues as well as nurses, assistants and all the members of the Institute.

Photocopies of essential publications